ADAMTS8 Promotes the Development of Pulmonary Arterial Hypertension and Right Ventricular Failure -A Possible Novel Therapeutic Target-

Junichi Omura[1]; Kimio Satoh[1]; Nobuhiro Kikuchi[1]; Taijyu Satoh[1]; Ryo Kurosawa[1]; Masamichi Nogi[1]; Tomohiro Ohtsuki[1]; Md Elias Al-Mamun[1]; Mohammad Abdul Hai Siddique[1], Nobuhiro Yaoita[1]; Shinichiro Sunamura[1]; Satoshi Miyata[1]; Yasushi Hoshikawa[2]; Yoshinori Okada[3]; Hiroaki Shimokawa[1]

[1]Department of Cardiovascular Medicine, Tohoku University Graduate School of Medicine, Sendai, Japan. [2]Department of Thoracic Surgery, Fujita Health University School of Medicine, Toyoake, Japan.[3]Department of Thoracic Surgery, Institute of Development, Aging and Cancer, Tohoku University, Sendai, Japan.

Running title: ADAMTS8 in Pulmonary Hypertension

Subject Terms:
Basic Science Research
Smooth Muscle Proliferation and Differentiation
Vascular Biology

Address correspondence to:
Dr. Hiroaki Shimokawa
Professor and Chairman
Department of Cardiovascular Medicine
Tohoku University Graduate School of Medicine
1-1 Seiryo-machi, Aoba-ku
Sendai 980-8574, Japan
Tel: +81-22-717-7153
shimo@cardio.med.tohoku.ac.jp

ABSTRACT

***Rationale*:** Pulmonary arterial hypertension (PAH) is characterized by pulmonary vascular remodeling with aberrant pulmonary artery smooth muscle cells (PASMCs) proliferation, endothelial dysfunction, and extracellular matrix remodeling.

Objective: Right ventricular (RV) failure is an important prognostic factor in PAH. Thus, we need to elucidate a novel therapeutic target in both PAH and RV failure.

***Methods and Results*:** We performed microarray analysis in PASMCs from patients with PAH (PAH-PASMCs) and controls. We found a disintegrin and metalloproteinase with thrombospondin motifs 8 (ADAMTS8), a secreted protein specifically expressed in the lung and the heart, was up-regulated in PAH-PASMCs and the lung in hypoxia-induced pulmonary hypertension (PH) in mice. To elucidate the role of ADAMTS8 in PH, we used vascular smooth muscle cell-specific ADAMTS8-knockout mice ($ADAMTS^{\Delta SM22}$). Hypoxia-induced PH was attenuated in $ADAMTS^{\Delta SM22}$ mice compared with controls. ADAMTS8 overexpression increased PASMC proliferation with downregulation of AMP-activated protein kinase (AMPK). In contrast, deletion of ADAMTS8 reduced PASMC proliferation with AMPK upregulation. Moreover, deletion of ADAMTS8 reduced mitochondrial fragmentation under hypoxia *in vivo* and *in vitro*. Indeed, PASMCs harvested from $ADAMTS^{\Delta SM22}$ mice demonstrated that phosphorylated dynamin-related protein 1 (DRP-1) at Ser637 was significantly up-regulated with higher expression of pro-fusion genes (*Mfn1* and *Mfn2*) and improved mitochondrial function. Moreover, recombinant ADAMTS8 induced endothelial dysfunction and matrix metalloproteinase activation in an autocrine/paracrine manner. Next, to elucidate the role of ADAMTS8 in RV function, we developed a cardiomyocyte-specific ADAMTS8 knockout mice ($ADAMTS8^{\Delta\alpha MHC}$). $ADAMTS8^{\Delta\alpha MHC}$ mice showed ameliorated RV failure in response to chronic hypoxia. In addition, $ADAMTS8^{\Delta\alpha MHC}$ mice showed enhanced angiogenesis and reduced RV ischemia and fibrosis. Finally, high-throughput screening revealed that mebendazole, which is used for treatment of parasite infections, reduced ADAMTS8 expression and cell proliferation in PAH-PASMCs and ameliorated PH and RV failure in PH rodent models.

***Conclusions*:** These results indicate that ADAMTS8 is a novel therapeutic target in PAH.

Keywords:

Hypoxia, inflammation, pulmonary hypertension, ADAMTS8.

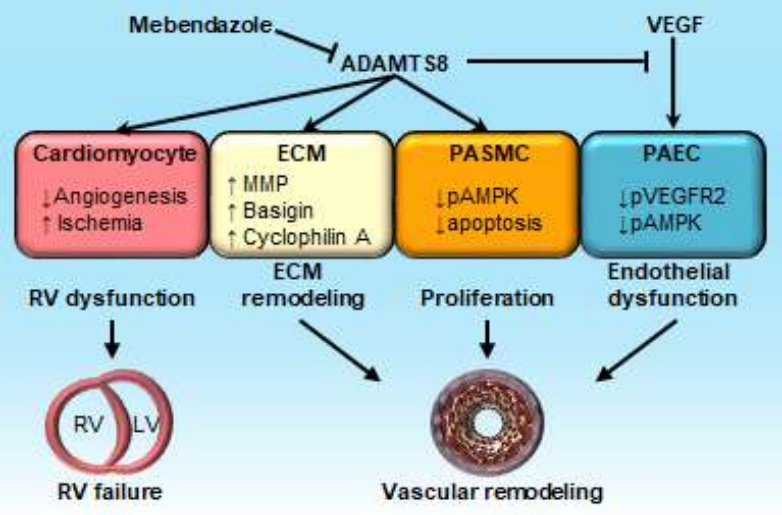

Nonstandard Abbreviations and Acronyms:

ADAMTS8	a disintegrin and metalloproteinase with thrombospondin motifs 8
AMPK	AMP-activated protein kinase
αSMA	α-smooth muscle actin
Bsg	basigin
CM	conditioned medium
CyPA	cyclophilin A
ECM	extracellular matrix
eNOS	endothelial nitric oxide synthase
FGF-2	fibroblast growth factor-2
NADPH	nicotinamide adenine dinucleotide phosphate
NO	nitric oxide
PAEC	pulmonary artery endothelial cell
PA	pulmonary artery
PH	pulmonary hypertension
PAH	pulmonary arterial hypertension
PASMC	pulmonary artery smooth muscle cell
PH	pulmonary hypertension
ROS	reactive oxygen species
RVH	right ventricular hypertrophy
RVSP	right ventricle systolic pressure

INTRODUCTION

Structural remodeling of pulmonary vessels is an important feature of pulmonary arterial hypertension (PAH) reflecting distal arterial muscularization and matrix remodeling.[1] PAH is a complex and progressive cardiopulmonary disorder with poor prognosis and no curative options. The pathogenesis of PAH involves many cell types (e.g., endothelial cells, vascular smooth muscle cells, and immune cells) and multiple factors (e.g., genetic background, DNA damage, hypoxia, and inflammation) that together affect many signaling pathways. Although many approaches to treatment of PAH have been developed over the past decades, the prognosis still remains poor.[2] Although several experimental studies have shown beneficial effects of several drugs with different mechanisms of action, the currently approved medication for PAH mainly focuses on dilating the remodeled pulmonary vessels.[1] Considering the complexity of the pathogenesis of PAH, it is reasonable to expect that diverse signaling pathways are involved, necessitating the development of comprehensive and integrative theories of the underlying mechanisms.

Right ventricular (RV) dysfunction is an important prognostic factor in PAH.[3] Indeed, RV failure is the main cause of death in PAH patients.[4] Additionally, post-capillary pulmonary hypertension (PH) is a major complication of left ventricular (LV) failure. RV dysfunction accompanied with elevated pulmonary artery (PA) pressure worsens the prognosis of LV failure dramatically.[5] Although insufficient angiogenesis in the setting of increased PA pressure induces RV ischemia and dysfunction, the detailed mechanism of the impaired RV angiogenesis in patients with PH remains elusive.[6] Thus, RV dysfunction has emerged as an important research priority in the cardiopulmonary research field. Here we hypothesized that unidentified pathogenic proteins strongly expressed in pulmonary artery smooth muscle cells of PAH patients (PAH-PASMCs) could promote PA remodeling and induce RV failure.

To identify novel pathogenic proteins, we performed microarray analyses using PAH-PASMCs and found significant up-regulation of a disintegrin and metalloproteinase with thrombospondin motifs 8 (ADAMTS8, encoded by the *ADAMTS8* gene) compared with control PASMCs. We further found that ADAMTS8, a secreted protein, was highly expressed in the lung of PAH patients, mice with hypoxia-induced PH, and rats with Sugen/hypoxia-induced PH. ADAMTS family proteins (ADAMTSs) are structurally and functionally similar to matrix metalloproteinases (MMPs) and a disintegrin and metalloproteinases (ADAMs).[7] Unlike ADAMs, which are membrane-anchored proteins, ADAMTSs are secreted proteinases binding to extracellular matrix (ECM).[8] Various ADAMTSs have been shown to regulate cell proliferation, adhesion, migration, and intracellular signaling.[7,8] Importantly, recent large-scale genome-wide association studies (GWASs) demonstrated that ADAMTS7 is a novel locus for coronary

atherosclerosis.[9] ADAMTS7 is ubiquitously expressed in many tissues, especially in the aortic walls. In contrast, ADAMTS8 is highly expressed in the lung and the heart.[10] It is also known that ADAMTS8 plays a crucial role in antiangiogenic responses.[10] In particular, ADAMTS8 regulates functional responses in cardiac tissues after myocardial infarction in rats.[11] However, the role of ADAMTS8 in the development of PAH remains to be elucidated.

To determine whether ADAMTS8 participates in the pathogenesis of PAH, we used a multidisciplinary translational approach. Here, we report that ADAMTS8 promotes proliferation of PASMCs, ECM remodeling, and endothelial dysfunction in an autocrine/paracrine manner. Using mice with PASMC-specific ADAMTS8 deficiency, we demonstrated a pathogenic role of ADAMTS8 in the development of hypoxia-induced PH. Additionally, using mice with cardiac-specific ADAMTS8 deficiency, we demonstrated a pathogenic role of ADAMTS8 in the development of RV dysfunction in hypoxia-induced PH. Finally, we discovered that mebendazole, an anthelmintic drug, reduces ADAMTS8 expression in PASMCs and their proliferation and ameliorates PH and RV dysfunction in rodent models of PH. Thus, our data suggest that ADAMTS8 could be a novel and feasible therapeutic target of PAH.

METHODS

The data that support the findings of this study are available from the corresponding author upon reasonable request. All experiments were performed in accordance with human and animal ethical guidelines in Tohoku University and Laval University. Additional detailed methods are available in the online-only Supplemental material.

Human lung samples.

Lung tissues were obtained from patients at the time of lung transplantation or surgery for lung cancer at a site far from the tumor margins. Lung tissues were obtained from PAH patients at the time of lung transplantation as previously described. All patients provided written informed consent for the use of their lung tissues for the present study.

Animal experiments.

All animal experiments were performed in accordance with the protocols approved by the Tohoku University Animal Care and Use Committee (No. 2015-Kodo-008) based on the ARRIVE trial (Animal

Research: Reporting of In Vivo Experiments) guideline. We performed all experiments with thorough randomization.

Statistical analyses.

All results are shown as mean±SEM. Comparisons of means between 2 groups were performed by unpaired Student's *t*-test or one-way analysis of variance (ANOVA) with interaction terms, followed by Tukey's HSD (honestly significant difference) for multiple comparisons. Comparisons of mean responses associated with the two main effects of the different genotypes and the severity of pulmonary vascular remodeling were performed by two-way ANOVA with interaction terms, followed by Tukey's HSD for multiple comparisons. Statistical significance was evaluated with JMP 12 (SAS Institute Inc., Cary, America) or R version 3.3.2 (http://www.R-project.org/). The time-dependent data were analyzed by repeated-measures linear mixed-effect model with lmer 1.1-12 and lmerTest 2.0-33 packages of R. The ratio of fully muscularized vessels was analyzed by the Poisson regression with the offset equals to the sum of total vessels with multcomp 1.4-6 package or R. All reported P values are 2-tailed, with a p value of less than 0.05 indicating statistical significance.

RESULTS

Screening for novel therapeutic targets in PAH.

To find novel therapeutic targets of PAH, we established cell libraries of primary cultured PASMCs from PAH patients undergoing lung transplantation and performed gene expression microarray analysis (**Figure 1A**). Among a total of 26,083 genes analyzed, the microarray analysis showed significant changes in 1,858 genes, which were up-regulated or down-regulated in PAH-PASMCs compared with control PASMCs (Figure 1B, SAM *t*-test P values of <0.05 and absolute values of logarithm of fold changes >1.0). We used the following selection criteria to identify relevant genes among the genes that showed significant changes in the microarray analysis; (1) up-regulation in PAH-PASMCs, (2) expression in the lung and the heart, (3) encoding of a secretory protein, and (4) encoding of a vascular regulatory protein. After rigorous analyses of the microarray data and previous publications, we finally selected ADAMTS8 from other genes (interleukin 6 receptor and clusterin) which met these criteria (Figure 1B). As ADAMTS8 has been reported as a secreted protein specifically expressed in the lung and the heart.[10] The structure of ADAMTS8 shares a common component with the structure of thrombospondin type 1 motif (TSP-1)

(Figure 1C). To confirm that ADAMTS8 is expressed in distal pulmonary arteries, we used lung tissues from PAH patients. Immunostaining showed that ADAMTS8 was strongly expressed in the thickened walls of distal pulmonary arteries in patients with from PAH (Figure 1D). Moreover, ADAMTS8 in αSMA-positive areas of distal pulmonary arteries was up-regulated in PAH patients (Figure 1E and online-only Data Supplement Figure I). In agreement, Western blot showed that the amount of ADAMTS8 was significantly increased in the lungs of PAH patients compared with those of controls (Figure 1F). Moreover, real-time PCR (RT-PCR) showed that the *ADAMTS8* gene was expressed more strongly in PAH-PASMCs than in control PASMCs (Figure 1G). Furthermore, protein levels of ADAMTS8 were significantly increased in PAH-PASMCs compared with control PASMCs (Figure 1H). On the other hand, there was no significant difference in the expression level of ADAMTS8 between control PAECs and PAH-PAECs (online-only Data Supplement Figure IIA). Furthermore, ADAMTS8 was equally expressed in both PAH-PAECs and PAH-PASMCs (online-only Data Supplement Figure IIB). Importantly, ADAMTS8 expression was specific to the lung and the heart, and hypoxia increased the ADAMTS8 protein level in the lung of wild-type mice (Figures 1I and 1J). In contrast, hypoxia reduced the ADAMTS8 protein level in the heart of wild-type mice (Figure 1K). These results suggest that ADAMTS8 in PASMCs may be involved in the development of PAH.

Targeted deletion of ADAMTS8 in PASMCs ameliorates hypoxia-induced PH.

To evaluate the specific role of ADAMTS8 in PASMCs, we developed a smooth muscle-specific ADAMTS8 knockout mouse (*ADAMTS8* $^{flox/flox}$*/Sm22a-cre*$^{+/-}$; ADAMTS8$^{\Delta SM22\alpha}$) (Figure 2A and online-only Data Supplement Figure III). ADAMTS8$^{\Delta SM22\alpha}$ and control (*ADAMTS8* $^{flox/flox}$*/Sm22α-cre*$^{-/-}$) mice showed normal growth under physiological conditions. Systolic blood pressure, diastolic blood pressure, heart rate, and body weight, as well as cardiac function assessed by echocardiography, were comparable between the two genotypes at baseline (Figure 2B and online-only Data Supplement Figure IV). Indeed, it has been reported that SM22α is also expressed in myeloid cells, including neutrophils, monocytes, and macrophages, in addition to smooth muscle cells.[12] It is reported that ADAMTS8 is expressed in macrophage.[13] It is also known that the myeloid cells play a crucial role in tissue homeostasis.[14,15] There was no difference in blood levels of total bilirubin (T-Bil), glutamate oxaloacetate transaminase (GOT), glutamate pyruvate transaminase (GPT), creatinine, or blood urea nitrogen (BUN) (online-only Data Supplement Figure V). Furthermore, ADAMTS8 levels in the lungs were significantly lower in ADAMTS8$^{\Delta SM22\alpha}$ mice than in control mice (online-only Data Supplement Figure VIA). The morphology of pulmonary arteries in normoxic ADAMTS8$^{\Delta SM22\alpha}$ mice did not differ from that of normoxic control mice (Figure 2C). In contrast, a significant difference in the medial thickness of pulmonary arteries was noted

after the animals were subjected to hypoxia for 4 weeks (Figure 2C). In particular, compared with control mice, ADAMTS8$^{\Delta SM22\alpha}$ mice showed fewer muscularized distal pulmonary arteries in response to hypoxia (Figure 2C). Muscularized distal pulmonary arteries exhibited immunoreactivity to αSMA (Figure 2C). Consistent with these morphological changes, control mice showed increased right ventricular systolic pressure (RVSP), which was attenuated in ADAMTS8$^{\Delta SM22\alpha}$ mice (Figure 2D). By contrast, systemic blood pressure was comparable between the two genotypes (online-only Data Supplement Figure VIB). The increased ratio of right ventricle to left ventricle plus septum weight (right ventricular hypertrophy, RVH) was also attenuated in ADAMTS8$^{\Delta SM22\alpha}$ mice (Figure 2E), suggesting a crucial role for ADAMTS8 in hypoxia-induced PH. These results indicate that ADAMTS8 in PASMCs plays a crucial role in the development of hypoxia-induced PH.

To further examine the possible role of ADAMTS8 in the development of PH *in vivo*, we performed mechanistic experiments using PASMCs *in vitro*. To evaluate the role of ADAMTS8 in PASMCs, we harvested PASMCs from ADAMTS8$^{\Delta SM22\alpha}$ and control mice. ADAMTS8 levels in primary cultured PASMCs were significantly lower in ADAMTS8$^{\Delta SM22\alpha}$ mice than in control mice (Figure 2F). Interestingly, *Adamts8*$^{-/-}$ PASMCs showed reduced proliferation compared with *Adamts8*$^{+/+}$ PASMCs in response to 5% fetal bovine serum (FBS) (Figure 2G). Additionally, a wound healing assay showed reduced cell migration in *Adamts8*$^{-/-}$ PASMCs compared with *Adamts8*$^{+/+}$ PASMCs (Figure 2H). These results demonstrate that ADAMTS8 promotes PASMC proliferation and migration.

ADAMTS8 affects cell cycle regulatory genes in PASMCs.

In light of the crucial role of ADAMTS8 as a secretory protein, we then evaluated the role of ADAMTS8 in intracellular signaling and cell cycle regulation using PASMCs and the human recombinant ADAMTS8 (hrADAMTS8) protein. Western blot analysis showed that *Adamts8*$^{-/-}$ PASMCs, compared with *Adamts8*$^{+/+}$ PASMCs, had increased phosphorylation of AMP-activated protein kinase (AMPK)/acetyl-CoA carboxylase (ACC) signaling, and reduced Bcl-2/Bax ratio, which resulted in decreased PCNA expression (Figure 3A). In line with this observation, the depletion of ADAMTS8 showed the up-regulation of the caspase-3 and the increased apoptosis in PASMCs (online-only Data Supplement Figure VIIA and VIIB). Moreover, the knockdown of ADAMTS8 increased AMPK phosphorylation, and down-regulated BCL-2/Bax ratio and PCNA levels in control and PAH-PASMCs (online-only Data Supplement Figure VIIC). Treatment of human PASMCs with hrADAMTS8 promoted cell proliferation in a dose-dependent manner (Figure 3B). Moreover, Western blot analysis showed that hrADAMTS8 treatment reduced phosphorylation of AMPK/ACC signaling (Figure 3C) and increased the Bcl-2/Bax ratio

(Figure 3D). To further examine the role of excess of ADAMTS8 in PASMCs, we overexpressed ADAMTS8 in human PASMCs using an ADAMTS8-encoding plasmid. Constitutive production of ADAMTS8 in PASMCs induced a 6-fold increase in the ADAMTS8 level compared with a control plasmid, leading to increased expression of nicotinamide adenine dinucleotide phosphate (NADPH) oxidase 4 (*NOX4*) and decreased expression of *CDKN1*B (a cell cycle regulator),[16] *BAX* (an apoptosis-related gene),[17] and *APLN,*[18] all of which were associated with the pathogenetic vascular cell phenotypes of PAH in the previous studies (Figure 3E). Moreover, the up-regulation of ADAMTS8 in PASMCs reduced phosphorylation of AMPK and increased the Bcl-2/Bax ratio and cell proliferation (online-only Data Supplement Figure VIII). In contrast, a knockdown of ADAMTS8 using siRNA decreased the expression of *NOX4* and increased the expression of *CDKN1B,* [19] *BAX,* [17] *BCL2L11* (Bim),[17] and *APLN,* [20] all of which were related to the reduced cell proliferation of PASMCs (Figure 3F). Moreover, ADAMTS8 siRNA markedly reduced proliferation of human PASMCs compared with control siRNA (**Figure 3G**). These results demonstrate that ADAMTS8 affects intracellular signaling and cell cycle regulatory genes in PASMCs.

ADAMTS8-mediated mitochondrial dysfunction in PASMCs.

Considering the importance of ADAMTS8 in PASMC proliferation and migration, we next focused on the role of ADAMTS8 in the ability of intracellular metabolism to tolerate the hyper-proliferative status. Recent studies have shown an emerging role of reactive oxygen species (ROS) and mitochondrial function in PASMC proliferation.[21] To examine the role of ADAMTS8 as a modulator of ROS and mitochondrial function in PASMCs, we used *Adamts8*$^{+/+}$ and *Adamts8*$^{-/-}$ PASMCs. 2,7-dichlorodihydrofluorescein (DCF) staining showed significantly lower levels of ROS in *Adamts8*$^{-/-}$ PASMCs than in *Adamts8*$^{+/+}$ PASMCs under hypoxia (Figure 4A). CellROX staining also showed significantly lower levels of ROS in *Adamts8*$^{-/-}$ PASMCs than in *Adamts8*$^{+/+}$ PASMCs under hypoxia (Figure 4B). In contrast, MitoSOX staining showed significantly higher levels of mitochondrial ROS in *Adamts8*$^{-/-}$ PASMCs than in *Adamts8*$^{+/+}$ PASMCs under the same condition (Figure 4C). Additionally, DCF and CellROX stainings showed significantly lower levels of ROS in control and PAH-PASMCs transfected with ADAMTS8 siRNA under both normoxia and hypoxia (online-only Data Supplement Figure IXA and B). MitoSOX staining showed significantly higher levels of mitochondrial ROS in control and PAH-PASMCs transfected with ADAMTS8 siRNA under the same condition (online-only Data Supplement Figure IXC). DHE staining of the lung produced consistent results, showing that hypoxic exposure increased ROS levels within autofluorescence of the elastic lamina in the distal pulmonary arteries in both genotypes (Figure 4D). However, the levels of ROS in pulmonary arteries were significantly less in

ADAMTS8$^{\Delta SM22\alpha}$ mice compared with control mice (Figure 4D). Recent studies have identified a mechanistic link between mitochondrial ROS production, mitochondrial morphology, and quality control *in vitro*.[22] Thus, we next examined mitochondrial morphology and networks using MitoTracker and transmission electron microscopy in *Adamts8*$^{+/+}$ and *Adamts8*$^{-/-}$ PASMCs. Interestingly, *Adamts8*$^{-/-}$ PASMCs showed less mitochondrial fragmentation than *Adamts8*$^{+/+}$ PASMCs after hypoxia (Figure 4E).

Thus, we next examined these molecules in the context of mitochondrial fission and fusion in *Adamts8*$^{+/+}$ and *Adamts8*$^{-/-}$ PASMCs. Interestingly, we found that protein level of DRP-1 and its phosphorylation level at Ser637 were significantly up-regulated in *Adamts8*$^{-/-}$ PASMCs compared with *Adamts8*$^{+/+}$ PASMCs (Figure 4F). RT-PCR showed that pro-fusion genes (*Mfn1* and *Mfn2*) were significantly up-regulated in *Adamts8*$^{-/-}$ PASMCs compared with *Adamts8*$^{+/+}$ PASMCs (Figure 4G). In contrast, expression of pro-fission genes (*Fis1* and *Mff*) was comparable in *Adamts8*$^{+/+}$ and *Adamts8*$^{-/-}$ PASMCs (Figure 4H). In agreement, transmission electron microscopy showed less mitochondrial fragmentation in *Adamts8*$^{-/-}$ PASMCs compared with *Adamts8*$^{+/+}$ PASMCs (online-only Data Supplement Figure X). Additionally, we found less mitochondrial fragmentation in pulmonary arterial walls of ADAMTS8$^{\Delta SM22\alpha}$ mice after 4 weeks of exposure to hypoxia (10% O_2) compared with control mice (Figure 4I). Moreover, the suppression of ADAMTS8 showed less mitochondrial fragmentation in addition to the up-regulated phosphorylated DRP-1 at Ser637 and pro-fusion genes in control and PAH-PASMCs after hypoxia (online-only Data Supplement Figure IXC-IXF). These results suggest that ADAMTS8 is one of the mechanistic explanations for the increased mitochondrial fragmentation in PAH-PASMCs. Using a Seahorse XF24-3 apparatus, which provides information on mitochondrial function through real-time measurements of oxygen consumption rate (OCR; a marker of oxidative phosphorylation) and extracellular acidification rate (ECAR; a surrogate for glycolysis), we examined hypoxia-induced responses in *Adamts8*$^{+/+}$ and *Adamts8*$^{-/-}$ PASMCs (online-only Data Supplement Figure XIA). OCR reflects the mitochondrial respiration rate and energy production and ECAR reflects the rate of glycolysis in PASMCs. Here, we observed significantly higher levels of OCR/ECAR ratio and maximal OCR in *Adamts8*$^{-/-}$ PASMCs compared with *Adamts8*$^{+/+}$ PASMCs (online-only Data Supplement Figure XIB). Moreover, hypoxic exposure reduced OCR and OCR/ECAR ratio compared with normoxia in both *Adamts8*$^{+/+}$ and *Adamts8*$^{-/-}$ PASMCs (online-only Data Supplement Figure XIB). These results suggest that ADAMTS8 is one of the mechanistic explanations for the mitochondrial dysfunction in PAH-PASMCs. Finally, *Adamts8*$^{-/-}$ PASMCs showed significantly lower levels of NADPH oxidase activity than *Adamts8*$^{+/+}$ PASMCs after hypoxia (Figure 4J). These results demonstrate that the balance between mitochondrial fission and fusion is regulated by ADAMTS8 in PASMCs (Supplemental Figure XII).

ADAMTS8 activates MMPs and perivascular inflammation.

ADAMTSs are secreted extracellular enzymes that degrade ECM. Degradation of ECM in turn affects other ECM enzymes. Thus, we next examined whether ADAMTS8 could influence other ECM enzymes, such as MMPs, cyclophilin A (CyPA), and its receptor basigin (Bsg).[23,24] Bsg is also known as extracellular MMP inducer (EMMPRIN), which binds to extracellular CyPA and activates MMPs.[25] In situ zymography showed that exogenous hrADAMTS8 treatment significantly activated MMPs in human PASMCs in a dose-dependent manner (Figure 5A). Western blotting also showed that MMP-2 and MMP-9 in PASMCs were up-regulated after hrADAMTS8 treatment (online-only Data Supplement Figure XIIIA). hrADAMTS8 also up-regulated MMP-12 and MMP13 (online-only Data Supplement Figure XIIIB). Additionally, Western blot showed that hrADAMTS8 treatment increased the secretion of CyPA and Bsg, both of which activate extracellular MMPs and vascular remodeling, in a dose-dependent manner (Figure 5B). To further evaluate the role of ADAMTS8 as a modulator of MMP activity in PASMCs, we used *Adamts8*$^{+/+}$ and *Adamts8*$^{-/-}$ PASMCs. Importantly, MMP activity assessed with DQ gelatin was significantly lower in *Adamts8*$^{-/-}$ PASMCs than in *Adamts8*$^{+/+}$ PASMCs under hypoxia (Figure 5C). This result was confirmed by *in situ* zymography (DQ gelatin), which demonstrated that hypoxia-induced MMP activation in the lung was significantly reduced in ADAMTS8$^{\Delta SM22\alpha}$ mice compared with control mice (Figure 5D). Moreover, MMP-2 induction by hypoxia was significantly weaker in the lungs of ADAMTS8$^{\Delta SM22\alpha}$ mice compared with control mice (Figure 5E). Since activation of MMPs promotes pulmonary vascular inflammation, we next examined the role of ADAMTS8 in hypoxia-induced inflammatory cell migration. As expected, hypoxia exacerbated perivascular inflammation in control mice, whereas ADAMTS8$^{\Delta SM22\alpha}$ mice showed reduced accumulation of perivascular Mac-3^{+} inflammatory cells in the lung (online-only Data Supplement Figure XIV). Thus, ADAMTS8 activates MMPs and exacerbates perivascular inflammation in an autocrine/paracrine manner (online-only Data Supplement Figure XV).

ADAMTS8-mediated interaction between PASMCs and PAECs.

We have recently demonstrated the crucial roles of the interaction between PASMCs and pulmonary artery endothelial cells (PAECs) in the development of PH.[26] In that study, we demonstrated the crucial role of endothelial AMPK/ACC signaling in pulmonary vascular homeostasis. Thus, we next assessed the effects of PASMC-derived ADAMTS8 on paracrine signaling of PAECs. Interestingly, hrADAMTS8 treatment significantly inhibited vascular endothelial growth factor (VEGF)-induced phosphorylation of VEGF receptor 2 (VEGFR2) in human PAECs (Figure 6A). Additionally, hrADAMTS8 treatment suppressed AICAR-induced phosphorylation of AMPK/ACC in human PAECs (Figure 6B).

Consistent with this result, hrADAMTS8 treatment significantly reduced PAEC proliferation in a dose-dependent manner (Figure 6C). Next, we prepared conditioned medium (CM) from human PASMCs transfected with an *ADAMTS8*-encoding plasmid (ADAMTS8-CM) or a control plasmid (control-CM) (Figure 6D). ADAMTS8-CM significantly inhibited VEGF-induced phosphorylation of VEGFR2 in human PAECs (online-only Data Supplement Figure XVIA). Treatment of human PAECs with ADAMTS8-CM significantly suppressed AMPK phosphorylation (Figure 6E), tube formation (Figure 6F), and cell proliferation (online-only Data Supplement Figure XVIB) in PAECs compared with treatment with control CM. Moreover, ADAMTS8-CM significantly increased ROS production in PAECs compared with control-CM (Figure 6G). In support of this result, RT-PCR analysis showed that ADAMTS8-CM increased expression of *BAX*, a pro-apoptotic factor, and reduced expression of *CCND1*, a cell-cycle promoter, and *APLN* (Apelin) in human PAECs compared with control-CM (Figure 6H). ADAMTS8-CM significantly decreased the Bcl-2/Bax ratio in addition to the tendency of suppressed apelin in PAECs treated with ADAMTS8-CM (online-only Data Supplement Figure XVIC). Furthermore, we also treated PAECs with CM from PAH-PASMCs (PAH-CM) (online-only Data Supplement Figure XVID). We found that treatment of PAH-CM on PAECs significantly suppressed AMPK phosphorylation and tube formation compared with that of CM from control PASMCs (online-only Data Supplement Figure XVIE and F). Moreover, PAH-CM significantly increased ROS production in PAECs compared with CM from control PASMCs (online-only Data Supplement Figure XVIG). qRT-PCR showed that PAH-CM up-regulated BAX and suppressed CCND1 and APLN (online-only Data Supplement Figure XVIH). Hence, these data suggested that the secretion of ADAMTS8 from PASMCs might be associated with the interaction between PAECs and PASMCs in the PAH pathogenesis. (Figure 6I).

Targeted deletion of ADAMTS8 in cardiomyocytes ameliorates RV failure in PH.

Since ADAMTS8 is also expressed in the heart, we developed a cardiomyocyte-specific ADAMTS8 knockout mouse (*ADAMTS8* $^{flox/flox}$*/aMHC-cre*$^{+/-}$; ADAMTS8$^{\Delta\alpha MHC}$) (Figure 7A). ADAMTS8$^{\Delta\alpha MHC}$ and control (*ADAMTS8* $^{flox/flox}$*/ aMHC-cre*$^{-/-}$) mice showed normal growth under physiological conditions. Systolic blood pressure, diastolic blood pressure, heart rate, and body weight, as well as cardiac function assessed by echocardiography, were comparable between the two genotypes at baseline (online-only Data Supplement Figure XVII). ADAMTS8 levels in the heart were significantly lower in ADAMTS8$^{\Delta\alpha MHC}$ mice than in control mice (Figure 7B). To further examine the role of myocardial ADAMTS8 in response to elevated PA pressure, we used hypoxia to induce PH in ADAMTS8$^{\Delta\alpha MHC}$ mice. After 4 weeks of hypoxia, there was no significant difference in RVSP or vascular remodeling between the two genotypes, whereas RVH was significantly reduced in ADAMTS8$^{\Delta\alpha MHC}$ mice compared with control

mice (Figure 7C and online-only Data Supplement Figure XVIII). Importantly, chronic hypoxia reduced the walking distance, evaluated using a treadmill, in control mice, and this effect was significantly ameliorated in ADAMTS8$^{\Delta\alpha MHC}$ mice (Figure 7D). Furthermore, echocardiography showed that ADAMTS8$^{\Delta\alpha MHC}$ mice had a significantly higher AcT/ET ratio, increased TAPSE, increased cardiac output, and reduced RVID compared with control mice after hypoxia for 4 weeks (Figure 7E and online-only Data Supplement Figure XIX). Moreover, sirius red staining showed significantly less RV fibrosis in ADAMTS8$^{\Delta\alpha MHC}$ mice than in control mice after chronic hypoxia (Figure 7F). Although immunostaining for CD31 showed that hypoxia increased capillary length and decreased capillary density, ADAMTS8$^{\Delta\alpha MHC}$ mice demonstrated reduced capillary length and higher capillary density in RVs than in RVs of control mice after hypoxic exposure (Figure 7G and online-only Data Supplement Figure XX). Consistently, staining with a hypoxic probe showed that ADAMTS8$^{\Delta\alpha MHC}$ mice had a smaller hypoxic area than control mice after hypoxia (Figure 7H). Finally, RT-PCR analysis showed significantly reduced expression of atrial natriuretic factor (ANF), brain natriuretic peptide (BNP), collagen 3a (Col3a), and glucose transporter type 4 (GLUT4) in RVs of ADAMTS8$^{\Delta\alpha MHC}$ mice than in RVs of control mice after chronic hypoxia (Figure 7I). These results demonstrate that ADAMTS8 in cardiomyocytes promotes the development of cardiac hypertrophy, fibrosis, and RV dysfunction in response to elevated RV pressure.

Mebendazole down-regulates ADAMTS8 and ameliorates PH and RV failure.

Given a key role of ADAMTS8 in pulmonary vascular remodeling and RV failure discovered in the present experiments above, we finally aimed to identify a therapeutic agent that can down-regulate ADAMTS8. An *in silico* screening using the Life Science Knowledge Bank (LSKB) software (http://www.lskb.w-fusionus.com/) identified several compounds as possible inhibitors of ADAMTS8. However, all these compounds were MMP inhibitors, which were shown to have serious side effects in preclinical trials.[27] Next, we used the public chemical library of the Drug Discovery Initiative (DDI) (http://www.ddi.u-tokyo.ac.jp/en/), a collection of 3,336 clinically used compounds and derivatives. A high-throughput screening identified 3 compounds that down-regulate ADAMTS8 expression and PAH-PASMC proliferation (Figure 8A). Among them, we focused on mebendazole (Figure 8B), which is used for treatment of parasite infections and has anti-proliferative effects against cancer cells.[28] We found that mebendazole treatment suppressed ADAMTS8 expression (Figure 8C) and proliferation of PAH-PAMSCs in a dose-dependent manner (Figure 8D). Mebendazole also suppressed control PASMC proliferation with the suppression of ADAMTS8. These data were consistent after ADAMTS8 in control PASMCs was overexpressed by ADAMTS8 plasmid (online-only Data Supplement Figure XXIA and XXIB). Furthermore, mebendazole treatment demonstrated down-regulation of PAH-PASMC proliferation after

the knockdown of ADAMTS8 by siRNA (online-only Data Supplement Figure XXIC and XXID). We then examined the effect of administration of mebendazole in hypoxia-induced PH in mice. Daily administration of mebendazole for 3 weeks had no effect on body weight, heart rate, or blood pressure compared with vehicle controls (online-only Data Supplement Figure XXIIA). Importantly, ADAMTS8 expression in the lung and the heart was significantly attenuated by mebendazole treatment (online-only Data Supplement Figures XXIIB and XXIIC). Moreover, mebendazole significantly suppressed muscularization of distal pulmonary arteries after hypoxic exposure (online-only Data Supplement Figure XXIID) and significantly reduced RVSP and RVH compared with vehicle control (online-only Data Supplement Figure XXIIE). Furthermore, mebendazole significantly reduced expression of ANF, Col3a, and GLUT4 in the RV (online-only Data Supplement Figure XXIIF). To further confirm the therapeutic potential of mebendazole in PAH, we used a rat model of PH induced by Sugen/hypoxia.[29] In this model, the levels of ADAMTS8 in the lung and RV were significantly elevated, which was inhibited by mebendazole treatment when started even after the development of PH (treatment protocol) (Figure 8E). To directly demonstrate the therapeutic effect of ADAMTS8 inhibition *in vivo*, rats were nebulized with ADAMTS8 siRNA after the establishment of PH (treatment protocol). Nebulization and inhalation of ADAMTS8 siRNA tended to reduce the protein levels of ADAMTS8 in the lungs of Sugen/hypoxia-induced PH rat model (online-only Data Supplement Figure XXIIIA and XXIIIB). Moreover, ADAMTS8 inhibition ameliorated PH and RV failure in rats *in vivo* (online-only Data Supplement Figure XXIIIC and XXIIID). Furthermore, mebendazole treatment significantly reduced RVSP, RVH (Figure 8F) and the wall thickness of distal pulmonary arteries compared with vehicle control treatment (Figure 8G). Echocardiography showed that mebendazole treatment increased AcT, TAPSE, cardiac output, and LVDd in addition to reduced RVID compared with vehicle control treatment (online-only Data Supplement Figure XXIV). Moreover, mebendazole treatment significantly increased capillary density in RV (Figure 8H), reduced RV fibrosis (Figure 8I), and increased walking distance (Figure 8J). These results demonstrate that mebendazole suppresses ADAMTS8 expression in the lung and RV and ameliorates PH and RV failure (Figure 8K).

DISCUSSION

The present study demonstrates that up-regulation of ADAMTS8 in PASMCs contributes to the pathogenesis of PAH, which involves proliferation and migration of PASMCs, enhanced MMP activity, and mitochondrial dysfunction. The present study also proposes ADAMTS8 inhibition in PASMCs as a novel strategy to prevent the development of PH. These conclusions are based on the following findings; (1) ADAMTS8 was up-regulated in PAH-PASMCs, (2) knockdown of ADAMTS8 in PASMCs attenuated

the development of hypoxia-induced PH in mice, (3) knockdown of ADAMTS8 reduced PASMC proliferation and migration, (4) ADAMTS8 reduced VEGF-induced PAEC proliferation and ameliorated endothelial function, (5) knockdown of ADAMTS8 in cardiomyocytes ameliorated the development of cardiac hypertrophy, fibrosis, and RV failure in response to elevated PA pressure, and (6) mebendazole treatment reduced ADAMTS8 expression in the lung and the RV and ameliorated PH and RV failure in rodents.

ADAMTS8 as a Novel Pathogenic Protein in PAH.

We utilized a translational multidisciplinary approach to find a novel pathogenic protein linking diverse signaling pathways that promote the development of PAH. ADAMTS8 was selected as a key protein involved in the pathogenesis of PAH based on analysis of 1,858 genes that were up-regulated or down-regulated in PAH-PASMCs. ADAMTSs are secreted proteins characterized by presence of an MMP domain and a variable number of TSP-1. Numerous studies have suggested a crucial role of MMP and TSP-1 in vascular homeostasis and vasculopathy, including PH.[30] Furthermore, various ADAMTSs have been shown to regulate cell proliferation, adhesion, migration, and intracellular signaling.[7,8] For example, ADAMTS1 deficiency induces thoracic aortic aneurysms and dissections in mice, while it is down-regulated in the aorta of patients with Marfan syndrome.[31] Moreover, the GWAS study demonstrated that ADAMTS7 is a novel locus for coronary artery disease in humans.[9] In support of this finding, ADAMTS7 deficiency suppressed neointimal formation after wire injury in mice and down-regulated migration of vascular smooth muscle cells.[32] It is also known that ADAMTS8 plays a crucial role in antiangiogenic responses.[10] Unlike ADAMTS1 and 7, both of which are ubiquitously expressed in various tissues, ADAMTS8 is specifically expressed in the lung and the heart.[10]

The molecular mechanisms in organogenesis and cellular differentiation is regulated by epigenetics in addition to genetics.[33] Additionally, the expression of ADAMTS8 in cancer cells was regulated by epigenetic modification.[34] The epigenetic modification may be involved in the selective tissue distribution of ADAMTS8. Consequently, it would be speculated that ADAMTS8 is implicated in the homeostasis of pulmonary vascular system rather than that of systemic vasculature. Indeed, ADAMTS8$^{\Delta SM22\alpha}$ mice did not show any phenotype in the vascular system except the attenuation of vascular remodeling in lung in response to hypoxia. Although we were unable to detect ADAMTS8 in the plasma in both PAH patients and controls, previous studies reported that ADAMTS8 is auto-catalytically and proteolytically cleaved just after secretion.[10,35] Moreover, other ADAMTS family proteins are auto-catalytically and proteolytically cleaved within its spacer region by matrix metalloproteinases.[36,37] Thus,

ADAMTS8 protein could be quickly degraded after the secretion in the local pulmonary vascular bed. Taken together, it is conceivable that the selective tissue distribution of ADAMTS8 may result in no apparent phenotypic changes in the vascular system except for the lung. At the same time, for the measurement of plasma levels of ADAMTS8, we may need further improvement of the method such as preparation and preservation after blood sampling. Although the analyses of circulating ADAMTS8 requires further investigation, our results raise the hypothesis that ADAMST8 plays a key role in the pathogenesis of PAH. According to the high-throughput transcription factor functional studies from the TRANSFAC® database (http://gene-regulation.com/pub/databases.html) and GeneCards® database (http://www.genecards.org/), ADAMTS8 expression is potentially regulated by binding of several transcription factors, such as forkhead box protein O1 (FOXO1), runt-related transcription factor 2 (RUNX2), and estrogen receptor 1 (ER1), to its promoter region. Previous studies have demonstrated that these transcription factors also regulate PAH-PASMC proliferation. Thus, it is possible that ADAMTS8 expression is up-regulated in PAH-PASMCs, at least in part, by these transcription factors.

ADAMTS8 induces ROS production and MMP activation.

ADAMTS8 degrades proteoglycans, which are key components of ECM.[35] ECM affects cellular behavior in physiological and pathological processes and provides structural support. ECM can sequester and locally release growth factors, such as epidermal growth factor (EGF) and transforming growth factor-β (TGF-β).[38] Thus, ECM remodeling through proteolytic degradation can release these growth factors, affecting cell proliferation and migration.[38] In the present study, exogenous hrADAMTS8 treatment promoted PASMC proliferation and up-regulated several ECM enzymes, including MMP-2, MMP-9, MMP-12, MMP-13. CyPA, and Bsg, all of which play crucial roles in the pathogenesis of PAH.[24,30,39,40] In contrast, ADAMTS8 deficiency down-regulated PASMC proliferation *in vitro* and ameliorated pulmonary vascular remodeling *in vivo,* which was accompanied by significant down-regulation of MMPs, CyPA, and Bsg in the lung. These results indicate that ADAMTS8 promotes ECM remodeling, PASMC proliferation, and development of PAH.

In addition to the ADAMTS8-induced ECM remodeling, we demonstrated that ADAMTS8 changed the intracellular metabolism in PASMCs, including AMPK signaling, apoptosis signaling, ROS levels, and mitochondrial function. ROS serve as important intracellular and intercellular messengers in a variety of signaling pathways that promote smooth muscle cell proliferation, migration, expression of proinflammatory mediators, and ECM remodeling. NOX4-induced ROS production activates hypoxia-inducible factor-1α (HIF-1α)[41] and HIF-2α in PASMCs.[42] HIFs suppress mitochondria-dependent apoptosis

and increase cell proliferation, which are hallmarks of PAH.[43] Moreover, NOX4 is up-regulated in PASMCs by hypoxia, as well as in the lungs of PAH patients.[44] Interestingly, NOX4-dependent activation of mammalian target of rapamycin complex 2 (mTORC2) promotes proliferative, apoptosis-resistant phenotypes of PAH-PASMC via down-regulation of AMPK signaling.[17] It is well known that AMPK regulates metabolism, which results in the suppression of anabolism to minimize ATP consumption and the acceleration of catabolism to stimulate ATP production.[45] Furthermore, the majority of ATP production in cells is regulated by TCA cycles. As expected, in addition to the up-regulation of AMPK signaling, *Adamts8*$^{-/-}$ PASMCs showed up-regulated basal OCR, which suggested increased ATP production. Moreover, genetic ablation of the AMPK in cancer cells promotes metabolic shift to glycolysis.[46] The suppression of AMPK signal and metabolic abnormality (i.e., suppression of mitochondrial glucose oxidation and increased glycolysis) are implicated in PAH pathogenesis including PASMCs.[17,47] These previous reports support the up-regulation of OCR/ECAR (metabolic shift from glycolysis to mitochondrial oxidation) in *Adamts8*$^{-/-}$ PASMCs, demonstrating increased AMPK signaling. In addition, previous reports showed that down-regulation of AMPK promoted cell proliferation in cancer cells and PASMC from PAH patients.[17,48] Activation of AMPK inhibits platelet derived growth factor (PDGF)-induced PASMC proliferation.[49] Indeed, *Adamts8*$^{-/-}$ PASMCs also showed reduced proliferation in response to 5% FBS. Thus, we consider that the up-regulation of metabolism (increased ATP production and metabolic shift to mitochondrial glucose oxidation) and the down-regulation of cell proliferation may be associated with the increased AMPK activity after the depletion of ADAMTS8 in PASMCs. AMPK also promotes mitochondrial biogenesis by activation of peroxisome proliferator-activated receptor γ coactivator-1α (PGC-1α).[50] PGC-1α is related to mitochondrial dynamics since it promotes MFN2, and PGC-1α-mediated down-regulation of MFN2 contributes to the mitochondrial fragmentation and excessive proliferation of PAH-PASMCs.[51] All these previous studies support our present findings that ADAMTS8 enhances NOX4-mediated ROS production and PASMC proliferation and down-regulates AMPK and apoptosis signaling. Moreover, genetic deletion of ADAMTS8 in PASMCs reduced hypoxia-mediated mitochondrial fragmentation. Thus, ADAMTS8 induces numerous intracellular signals by activation of extracellular MMPs and resultant NOX4-mediated ROS production in PAH-PASMCs.

ADAMTS8 causes endothelial dysfunction in an autocrine/paracrine manner.

An initial loss of PAECs as a result of environmental stresses (e.g., hypoxia, inflammation, and SU5416) is recognized as the first step of vascular remodeling in the pathogenesis of PAH.[26,29] In the present study, exogenous hrADAMTS8 down-regulated the VEGF/VEGFR2 pathway in PAECs and impaired endothelial function. These results were consistent with the previous studies demonstrating that ADAMTS8

down-regulates VEGF-induced angiogenesis and cell proliferation in human dermal ECs.[10] ADAMTS1 has anti-angiogenic properties since it binds to VEGF-A and negatively modulates VEGF function in ECs via TSP-1 motifs. Thus, it is possible that ADAMTS8 down-regulates the VEGF/VEGFR2 pathway using its TSP-1 motifs. We also demonstrated that hrADAMTS8 and ADAMTS8-CM down-regulated AMPK signalling in PAECs. Our data are consistent with previous reports demonstrating that AMPK in PAECs is regulated by VEGF signaling.[52] Moreover, ADAMTS8-CM significantly increased ROS levels in PAECs and inhibited angiogenesis via increased expression of *BAX* and reduced expression of *CCND1*. It is known that AMPK plays an important role in endothelial function and vascular homeostasis through several mechanisms, including endothelial nitric oxide synthase (eNOS), anti-apoptotic effect, and ROS regulation in PAECs.[26] Taken together, these data indicate that ADAMTS8 secreted from adjacent PASMCs induces endothelial dysfunction in an autocrine/paracrine manner through down-regulation of the VEGFR2/AMPK signaling. Our data suggest that the up-regulation of ADAMTS8 in PASMCs could exacerbate the phenotype of PAH-PASMC, endothelial dysfunction, and extracellular matrix remodeling in an autocrine/paracrine manner. Hence, these integrated effects caused by the up-regulation of ADAMTS8 in PASMCs will promote the pathogenesis of PAH.

ADAMTS8 promotes RV fibrosis and failure.

To explore the role of ADAMTS8 in the RV, we used αMHC-Cre–mediated ADAMTS8-knockout. According to the validated protein expression studies from the Human Protein Atlas portal (www.proteinatlas.org), αMHC is also expressed in skeletal muscle in addition to higher expression in the heart. There was no study which examined the role of αMHC in skeletal muscle. Additionally, there was no research showing the expression of ADATMS8 in skeletal muscle in humans. We demonstrated that ADAMTS8$^{\Delta\alpha MHC}$ mice showed normal cardiac function and excise capacity under normoxia. These data suggest that there was no obvious influence on skeletal muscle in response to αMHC-Cre–mediated ADAMTS8-depletion under normoxia. Thus, these data indicate that ADAMTS8$^{\Delta\alpha MHC}$ mice did not show any phenotypic change under physiological conditions. The hypoxic ADAMTS8$^{\Delta\alpha MHC}$ mice showed improved RV function and reduced RVH compared with hypoxic control mice, whereas vascular remodeling and RVSP were comparable between the two genotypes in response to hypoxia Indeed, by using a pulmonary artery banding model, it was clearly demonstrated that both pharmacological and genetic approaches reduced RVH and improved RV function without any effects on RVSP.[53,54] Thus, our present findings indicate that loss of ADAMTS8 in cardiomyocytes had no effect on vascular remodeling and PH, but diminished RVH and improved RV function. Furthermore, ADAMTS8$^{\Delta\alpha MHC}$ mice showed reduced capillary length compared with control mice after hypoxic exposure. These results are consistent with the

previous studies demonstrating that capillary length in the RV is highly correlated with RV volume in animal models of PH and PAH patients.[55-57] Consistently, ADAMTS8$^{\Delta\alpha MHC}$ mice showed increased capillary density after hypoxia. This may suggest a passive change in inter-capillary distance due to reduced RV volume. Interestingly, ADAMTS8$^{\Delta\alpha MHC}$ mice also showed less myocardial ischemia and GLUT4 expression in the RV. Increased expression of GLUT4 in the RV suggests a metabolic switch to glycolysis, which is a strong indicator of RV dysfunction in animal models of PH and patients with PAH.[58,59] Here, ADAMTS8 inhibits VEGF-induced angiogenesis *in vitro*.[10] Additionally, VEGF in RV was up-regulated after hypoxia-induced PH in mice.[60] Moreover, VEGF-induced angiogenesis improved RV function in monocrotaline-induced PH and Sugen/hypoxia-induced PH in rats.[61,62] In contrast, insufficient angiogenesis in the setting of RVH induces ischemia and fibrosis in RV.[61] Therefore, down-regulation of ADAMTS8 can exert protective effects on the RV as well. Accordingly, it is speculated that the down-regulation of ADMTS8 in the RV from wild-type mice showed the cardioprotective effect against RV dysfunction in hypoxia-induced PH model. Consequently, it is convincible that in the cardiomyocyte-specific ADAMTS8-knockout mice, the complete depletion of ADAMTS8 in cardiomyocyte prevented its pathogenic effects on fibrotic change in the RV and resulted in the attenuation of RV failure in hypoxia-induced PH.

Mebendazole in drug repositioning.

The traditional approach to drug discovery involves identification and validation of new molecular entities, which is a time-consuming and costly process. More than 80% of new compounds ultimately fail in human studies even if they show beneficial effects in pre-clinical studies. The high failure rates and costs involved in the development of new drugs led to an increased interest in drug repositioning, the process of identifying new indications for existing drugs. Using a high-throughput screening of 3,336 compounds, including drugs and bioactive compounds, and further validation studies, we identified mebendazole as a potent ADAMTS8 inhibitor. Mebendazole is the most widely used drug for treating patients with helminth infestation owing to high efficacy, few side effects, and low cost. These characteristics can be beneficial if mebendazole is to be used as a novel agent for PAH therapy as an ADAMTS8 inhibitor. Additionally, we found that mebendazole ameliorated hypoxia-induced PH in mice and Sugen/hypoxia-induced PH in rats by down-regulating ADAMTS8 in the lungs and the RV. Recent studies reported that mebendazole down-regulates cell proliferation in several cancers.[28] Mebendazole is currently in clinical trials for cancer (NCT01729260 and NCT01837862), and no toxicity has been reported so far. Thus, mebendazole may be a promising agent, and a possibility of drug repositioning for use in patients with PAH needs to be explored.

Study limitations.

The present study has several limitations. First, ADAMTS8 was associated with cancer development in the previous study.[63] Moreover, there were several reports that demonstrated that PAH-PASMCs share several features with cancer cells, including hyperproliferation and resistance to apoptosis[4,59,64]. Thus, ADAMTS8 could be regulated by the underlying pathological mechanism that gives cancer-like phenotype in PAH-PASMCs. Second, we used SM22α as a driver for the tissue-specific expression in the vascular smooth muscle cells in the present study, however, it is known that SM22α is expressed not only in the vascular smooth muscle cells but also in the myeloid cells. It is also reported that ADAMTS8 is expressed in macrophages.[13] Myeloid cells, including neutrophils, monocytes, and macrophages, promote inflammation and exacerbate vascular remodeling in the pathogenesis of PAH. Given that the SM22α is expressed in these cells, we need to consider the possible involvement of hematopoietic subsets, including neutrophils, monocytes, and macrophages, in the phenotype of SM22α-Cre-mediated ADAMTS8-knockout mice under hypoxia. Third, we did not use tamoxifen-inducible models for time-specific ADAMTS8 knockout. However, ADAMTS8$^{\Delta SM22\alpha}$ and ADAMTS$^{8\Delta\alpha MHC}$ mice showed normal growth and normal phenotypes under normoxia. There is no data suggesting that SM22α or αMHC-Cre-mediated ADAMTS8-depletion created lethal phenotypes in embryos or pups. Thus, these data suggest that the role of ADAMTS8 in hypoxia-induced PH is sufficiently elucidated without tamoxifen induction model. Finally, the beneficial effects of mebendazole may involve several mechanisms other than down-regulation of ADAMTS8. Indeed, mebendazole suppressed vascular smooth muscle cell proliferation and attenuated neointimal formation following arterial injury in mice. Mebendazole regulates several intracellular molecules, including those involved in hedgehog signaling.[65] Additionally, mebendazole suppressed vascular smooth muscle cell proliferation and attenuated neointimal formation following arterial injury in mice.[66] Thus, further study is needed to elucidate the mechanism of the therapeutic effects of mebendazole. Thus, further study is needed to elucidate the mechanism of the therapeutic effects of mebendazole.

Clinical implication and conclusions.

Despite the rapid progress in the therapy of PAH in the last decade, there is still no cure for this devastating disease. This is largely attributable to the fact that various cell types and diverse signaling pathways induce vascular remodeling and RV dysfunction in PAH.[6] It is now widely accepted that epigenetic modifications are key factors in cancer and PAH following environmental stimuli (e.g., hypoxia and infection).[64] DNA methylation is a common epigenetic modification. In particular, previous studies

reported methylation of the *ADAMTS8* gene in cancer cells.[67] Furthermore, epigenetic modification can be modulated by SNPs, as has been clearly illustrated in a recent study on ADAMTS7 in coronary atherosclerosis.[68] Thus, genome screening for the *ADAMTS8* gene and ADAMTS8-associated genes can be beneficial for PAH patients.

In conclusion, the present study demonstrates that ADAMTS8 promotes vascular remodeling and RV failure in PAH patients and thus could be a novel therapeutic target of the disorder, for which mebendazole may be a therapeutic agent.

ACKNOWLEDGMENTS

We are grateful to the laboratory members in the Department of Cardiovascular Medicine of the Tohoku University for valuable technical assistance, especially to Yumi Watanabe, Ai Nishihara, and Hiromi Yamashita.

SOURCES OF FUNDING

This work was supported in part by the grants-in-aid for Scientific Research (15H02535, 15H04816, and 15K15046) from the Ministry of Education, Culture, Sports, Science and Technology, Tokyo, Japan, the grants-in-aid for Scientific Research from the Ministry of Health, Labour, and Welfare, Tokyo, Japan (10102895), and the grants-in-aid for Scientific Research from the Japan Agency for Medical Research and Development, Tokyo, Japan (15ak0101035h0001, 16ek0109176h0001, 17ek0109227h0001).

DISCLOSURES

None.

REFERENCES

1. Rabinovitch M. Molecular pathogenesis of pulmonary arterial hypertension. ***J Clin Invest***. 2012;122:4306-4313.

2. Michelakis ED. Pulmonary arterial hypertension: yesterday, today, tomorrow. ***Circ Res***. 2014;115:109-114.

3. van de Veerdonk MC, Kind T, Marcus JT, Mauritz GJ, Heymans MW, Bogaard HJ, Boonstra A, Marques KM, Westerhof N, Vonk-Noordegraaf A. Progressive right ventricular dysfunction in patients with pulmonary arterial hypertension responding to therapy. ***J Am Coll Cardiol***. 2011;58:2511-2519.

4. Ryan JJ, Archer SL. Emerging concepts in the molecular basis of pulmonary arterial hypertension: part I: metabolic plasticity and mitochondrial dynamics in the pulmonary circulation and right ventricle in pulmonary arterial hypertension. ***Circulation***. 2015;131:1691-1702.

5. Gulati A, Ismail TF, Jabbour A, Alpendurada F, Guha K, Ismail NA, Raza S, Khwaja J, Brown TD, Morarji K, Liodakis E, Roughton M, Wage R, Pakrashi TC, Sharma R, Carpenter JP, Cook SA, Cowie MR, Assomull RG, Pennell DJ, Prasad SK. The prevalence and prognostic significance of right ventricular systolic dysfunction in nonischemic dilated cardiomyopathy. ***Circulation***. 2013;128:1623-1633.

6. Ryan JJ, Archer SL. The right ventricle in pulmonary arterial hypertension: disorders of metabolism, angiogenesis and adrenergic signaling in right ventricular failure. ***Circ Res***. 2014;115:176-188.

7. Rodriguez-Manzaneque JC, Fernandez-Rodriguez R, Rodriguez-Baena FJ, Iruela-Arispe ML. ADAMTS proteases in vascular biology. ***Matrix Biol***. 2015;44-46:38-45.

8. Rocks N, Paulissen G, El Hour M, Quesada F, Crahay C, Gueders M, Foidart JM, Noel A, Cataldo D. Emerging roles of ADAM and ADAMTS metalloproteinases in cancer. ***Biochimie***. 2008;90:369-379.

9. Reilly MP, Li M, He J, Ferguson JF, Stylianou IM, Mehta NN, Burnett MS, Devaney JM, Knouff CW, Thompson JR, Horne BD, Stewart AF, Assimes TL, Wild PS, Allayee H, Nitschke PL, Patel RS, Myocardial Infarction Genetics C, Wellcome Trust Case Control C, Martinelli N, Girelli D, Quyyumi AA, Anderson JL, Erdmann J, Hall AS, Schunkert H, Quertermous T, Blankenberg S, Hazen SL, Roberts R, Kathiresan S, Samani NJ, Epstein SE, Rader DJ. Identification of ADAMTS7 as a novel locus for coronary atherosclerosis and association of ABO with myocardial infarction in the presence of coronary atherosclerosis: two genome-wide association studies. ***Lancet***. 2011;377:383-392.

10. Vázquez F, Hastings G, Ortega M, Lane T, Oikemus S, Lombardo M, Iruela-Arispe M. METH-1, a human ortholog of ADAMTS-1, and METH-2 are members of a new family of proteins with angio-inhibitory activity. ***J Biol Chem***. 1999 274:23349-23357.

11. Zhao C, Zha Y, Wu X, Chen L, Shi J, Cui L. The quantification of ADAMTS4 and 8 expression and selection of reference genes for quantitative real-time PCR analysis in myocardial infarction. ***Biomed Pharmacother***. 2011;65:555-559.

12. Shen Z, Li C, Frieler RA, Gerasimova AS, Lee SJ, Wu J, Wang MM, Lumeng CN, Brosius III FC, Duan SZ, Mortensen RM. Smooth muscle protein 22a -Cre is expressed in myeloid cells in mice. ***Biochem Biophys Res Commun***. 2012;422:639-642.

13. Wagsater D, Bjork H, Zhu C, Bjorkegren J, Valen G, Hamsten A, Eriksson P. ADAMTS-4 and -8 are inflammatory regulated enzymes expressed in macrophage-rich areas of human atherosclerotic plaques. ***Atherosclerosis***. 2008;196:514-522.

14. Munro DAD, Hughes J. The origins and functions of tissue-resident macrophages in kidney development. ***Front Physiol***. 2017;8:837.

15. Krenkel O, Tacke F. Liver macrophages in tissue homeostasis and disease. ***Nat Rev Immunol***. 2017;17:306-321.

16. Kikuchi N, Satoh K, Kurosawa R, Yaoita N, Elias-Al-Mamun M, Siddique MAH, Omura J, Satoh T, Nogi M, Sunamura S, Miyata S, Saito Y, Hoshikawa Y, Okada Y, Shimokawa H. Selenoprotein P promotes the development of pulmonary arterial hypertension. ***Circulation***. 2018;138:600-623.

17. Goncharov DA, Kudryashova TV, Ziai H, Ihida-Stansbury K, DeLisser H, Krymskaya VP, Tuder RM, Kawut SM, Goncharova EA. Mammalian target of rapamycin complex 2 (mTORC2) coordinates pulmonary artery smooth muscle cell metabolism, proliferation, and survival in pulmonary arterial hypertension. ***Circulation***. 2014;129:864-874.

18. Alastalo TP, Li M, Perez Vde J, Pham D, Sawada H, Wang JK, Koskenvuo M, Wang L, Freeman BA, Chang HY, Rabinovitch M. Disruption of PPARg/b-catenin-mediated regulation of apelin impairs BMP-induced mouse and human pulmonary arterial EC survival. ***J Clin Invest***. 2011;121:3735-3746.

19. Weiss A, Neubauer MC, Yerabolu D, Kojonazarov B, Schlueter BC, Neubert L, Jonigk D, Baal N, Ruppert C, Dorfmuller P, Pullamsetti SS, Weissmann N, Ghofrani H-A, Grimminger F, Seeger W,

Schermuly RT. Targeting cyclin-dependent kinases for the treatment of pulmonary arterial hypertension. ***Nature Communications***. 2019;10:2204.

20. Guignabert C, Alvira CM, Alastalo TP, Sawada H, Hansmann G, Zhao M, Wang L, El-Bizri N, Rabinovitch M. Tie2-mediated loss of peroxisome proliferator-activated receptor-γ in mice causes PDGF receptor-β-dependent pulmonary arterial muscularization. ***Am J Physiol Lung Cell Mol Physiol***. 2009;297:L1082-L1090.

21. Archer SL. Mitochondrial dynamics–mitochondrial fission and fusion in human diseases. ***N Engl J Med***. 2013;369:2236-2251.

22. Frank M, Duvezin-Caubet S, Koob S, Occhipinti A, Jagasia R, Petcherski A, Ruonala MO, Priault M, Salin B, Reichert AS. Mitophagy is triggered by mild oxidative stress in a mitochondrial fission dependent manner. ***Biochim Biophys Acta***. 2012;1823:2297-2310.

23. Satoh K, Nigro P, Matoba T, O'Dell MR, Cui Z, Shi X, Mohan A, Yan C, Abe J, Illig KA, Berk BC. Cyclophilin A enhances vascular oxidative stress and the development of angiotensin II-induced aortic aneurysms. ***Nat Med***. 2009;15:649-656.

24. Satoh K, Satoh T, Kikuchi N, Omura J, Kurosawa R, Suzuki K, Sugimura K, Aoki T, Nochioka K, Tatebe S, Miyamichi-Yamamoto S, Miura M, Shimizu T, Ikeda S, Yaoita N, Fukumoto Y, Minami T, Miyata S, Nakamura K, Ito H, Kadomatsu K, Shimokawa H. Basigin mediates pulmonary hypertension by promoting inflammation and vascular smooth muscle cell proliferation. ***Circ Res***. 2014;115:738-750.

25. Satoh K. Cyclophilin A in cardiovascular homeostasis and diseases. ***Tohoku J Exp Med***. 2015;235:1-15.

26. Omura J, Satoh K, Kikuchi N, Satoh T, Kurosawa R, Nogi M, Otsuki T, Kozu K, Numano K, Suzuki K, Sunamura S, Tatebe S, Aoki T, Sugimura K, Miyata S, Hoshikawa Y, Okada Y, Shimokawa H. Protective roles of endothelial AMP-activated protein kinase against hypoxia-induced pulmonary hypertension in mice. ***Circ Res***. 2016;119:197-209.

27. Vandenbroucke RE, Libert C. Is there new hope for therapeutic matrix metalloproteinase inhibition? ***Nat Rev Drug Discov***. 2014;13:904-927.

28. Bai RY, Staedtke V, Aprhys CM, Gallia GL, Riggins GJ. Antiparasitic mebendazole shows survival benefit in 2 preclinical models of glioblastoma multiforme. ***Neuro Oncol***. 2011;13:974-982.

29. Abe K, Toba M, Alzoubi A, Ito M, Fagan KA, Cool CD, Voelkel NF, McMurtry IF, Oka M. Formation of plexiform lesions in experimental severe pulmonary arterial hypertension. ***Circulation***. 2010;121:2747-2754.

30. Chelladurai P, Seeger W, Pullamsetti SS. Matrix metalloproteinases and their inhibitors in pulmonary hypertension. ***Eur Respir J***. 2012;40:766-782.

31. Oller J, Mendez-Barbero N, Ruiz EJ, Villahoz S, Renard M, Canelas LI, Briones AM, Alberca R, Lozano-Vidal N, Hurle MA, Milewicz D, Evangelista A, Salaices M, Nistal JF, Jimenez-Borreguero LJ, De Backer J, Campanero MR, Redondo JM. Nitric oxide mediates aortic disease in mice deficient in the metalloprotease Adamts1 and in a mouse model of Marfan syndrome. ***Nat Med***. 2017;23:200-212.

32. Kessler T, Zhang L, Liu Z, Yin X, Huang Y, Wang Y, Fu Y, Mayr M, Ge Q, Xu Q, Zhu Y, Wang X, Schmidt K, de Wit C, Erdmann J, Schunkert H, Aherrahrou Z, Kong W. ADAMTS-7 inhibits re-endothelialization of injured arteries and promotes vascular remodeling through cleavage of thrombospondin-1. ***Circulation***. 2015;131:1191-1201.

33. Skinner MK. Role of epigenetics in developmental biology and transgenerational inheritance. ***Birth Defects Res C Embryo Today***. 2011;93:51-55.

34. Choi GC, Li J, Wang Y, Li L, Zhong L, Ma B, Su X, Ying J, Xiang T, Rha SY, Yu J, Sung JJ, Tsao SW, Chan AT, Tao Q. The metalloprotease ADAMTS8 displays antitumor properties through antagonizing EGFR-MEK-ERK signaling and is silenced in carcinomas by CpG methylation. ***Mol Cancer Res***. 2014;12:228-238.

35. Collins-Racie LA, Flannery CR, Zeng W, Corcoran C, Annis-Freeman B, Agostino MJ, Arai M, DiBlasio-Smith E, Dorner AJ, Georgiadis KE, Jin M, Tan XY, Morris EA, LaVallie ER. ADAMTS-8

exhibits aggrecanase activity and is expressed in human articular cartilage. ***Matrix Biol***. 2004;23:219-230.

36. Liu Y-j, Xu Y, Yu Q. Full-length ADAMTS-1 and the ADAMTS-1 fragments display pro- and antimetastatic activity, respectively. ***Oncogene***. 2005;25:2452-2467.

37. Flannery CR, Zeng W, Corcoran C, Collins-Racie LA, Chockalingam PS, Hebert T, Mackie SA, McDonagh T, Crawford TK, Tomkinson KN, LaVallie ER, Morris EA. Autocatalytic cleavage of ADAMTS-4 (Aggrecanase-1) reveals multiple glycosaminoglycan-binding sites. ***J Biol Chem***. 2002;277:42775-42780.

38. Hynes RO. The extracellular matrix: not just pretty fibrils. ***Science***. 2009;326:1216-1219.

39. Herget J, Novotna J, Bibova J, Povysilova V, Vankova M, Hampl V. Metalloproteinase inhibition by Batimastat attenuates pulmonary hypertension in chronically hypoxic rats. ***Am J Physiol Lung Cell Mol Physiol***. 2003;285:L199-208.

40. Pullamsetti S, Krick S, Yilmaz H, Ghofrani HA, Schudt C, Weissmann N, Fuchs B, Seeger W, Grimminger F, Schermuly RT. Inhaled tolafentrine reverses pulmonary vascular remodeling via inhibition of smooth muscle cell migration. ***Respir Res***. 2005;6:128.

41. Diebold I, Petry A, Hess J, Gorlach A. The NADPH oxidase subunit NOX4 is a new target gene of the hypoxia-inducible factor-1. ***Mol Biol Cell***. 2010;21:2087-2096.

42. Diebold I, Flugel D, Becht S, Belaiba RS, Bonello S, Hess J, Kietzmann T, Gorlach A. The hypoxia-inducible factor-2α is stabilized by oxidative stress involving NOX4. ***Antioxid Redox Signal***. 2010;13:425-436.

43. Marsboom G, Wietholt C, Haney CR, Toth PT, Ryan JJ, Morrow E, Thenappan T, Bache-Wiig P, Piao L, Paul J, Chen CT, Archer SL. Lung ^{18}F-fluorodeoxyglucose positron emission tomography for diagnosis and monitoring of pulmonary arterial hypertension. ***Am J Respir Crit Care Med***. 2012;185:670-679.

44. Mittal M, Roth M, Konig P, Hofmann S, Dony E, Goyal P, Selbitz AC, Schermuly RT, Ghofrani HA, Kwapiszewska G, Kummer W, Klepetko W, Hoda MA, Fink L, Hanze J, Seeger W, Grimminger F, Schmidt HH, Weissmann N. Hypoxia-dependent regulation of nonphagocytic NADPH oxidase subunit NOX4 in the pulmonary vasculature. ***Circ Res***. 2007;101:258-267.

45. Herzig S, Shaw RJ. AMPK: guardian of metabolism and mitochondrial homeostasis. ***Nat Rev Mol Cell Biol***. 2018;19:121-135.

46. Faubert B, Boily G, Izreig S, Griss T, Samborska B, Dong Z, Dupuy F, Chambers C, Fuerth BJ, Viollet B, Mamer OA, Avizonis D, DeBerardinis RJ, Siegel PM, Jones RG. AMPK is a negative regulator of the Warburg effect and suppresses tumor growth in vivo. ***Cell Metab***. 2013;17:113-124.

47. Sutendra G, Michelakis ED. The metabolic basis of pulmonary arterial hypertension. ***Cell Metab***. 2014;19:558-573.

48. Hawley SA, Ross FA, Gowans GJ, Tibarewal P, Leslie NR, Hardie DG. Phosphorylation by Akt within the ST loop of AMPK-α1 down-regulates its activation in tumour cells. ***Biochem J***. 2014;459:275-287.

49. Song Y, Wu Y, Su X, Zhu Y, Liu L, Pan Y, Zhu B, Yang L, Gao L, Li M. Activation of AMPK inhibits PDGF-induced pulmonary arterial smooth muscle cells proliferation and its potential mechanisms. ***Pharmacol Res***. 2016;107:117-124.

50. Canto C, Gerhart-Hines Z, Feige JN, Lagouge M, Noriega L, Milne JC, Elliott PJ, Puigserver P, Auwerx J. AMPK regulates energy expenditure by modulating NAD^+ metabolism and SIRT1 activity. ***Nature***. 2009;458:1056-1060.

51. Ryan JJ, Marsboom G, Fang YH, Toth PT, Morrow E, Luo N, Piao L, Hong Z, Ericson K, Zhang HJ, Han M, Haney CR, Chen CT, Sharp WW, Archer SL. PGC1a-mediated mitofusin-2 deficiency in female rats and humans with pulmonary arterial hypertension. ***Am J Respir Crit Care Med***. 2013;187:865-878.

52. Stahmann N, Woods A, Spengler K, Heslegrave A, Bauer R, Krause S, Viollet B, Carling D, Heller R. Activation of AMP-activated protein kinase by vascular endothelial growth factor mediates endothelial angiogenesis independently of nitric-oxide synthase. ***J Biol Chem***. 2010;285:10638-10652.

53. Shi L, Kojonazarov B, Elgheznawy A, Popp R, Dahal BK, Bohm M, Pullamsetti SS, Ghofrani HA, Godecke A, Jungmann A, Katus HA, Muller OJ, Schermuly RT, Fisslthaler B, Seeger W, Fleming I. miR-223-IGF-IR signaling in hypoxia- and load-induced right-ventricular failure: a novel therapeutic approach. ***Cardiovasc Res***. 2016;111:184-193.

54. Ikeda S, Satoh K, Kikuchi N, Miyata S, Suzuki K, Omura J, Shimizu T, Kobayashi K, Kobayashi K, Fukumoto Y, Sakata Y, Shimokawa H. Crucial role of Rho-kinase in pressure overload-induced right ventricular hypertrophy and dysfunction in mice. ***Arterioscler Thromb Vasc Biol***. 2014;34:1260-1271.

55. Graham BB, Kumar R, Mickael C, Kassa B, Koyanagi D, Sanders L, Zhang L, Perez M, Hernandez-Saavedra D, Valencia C, Dixon K, Harral J, Loomis Z, Irwin D, Nemkov T, D'Alessandro A, Stenmark KR, Tuder RM. Vascular Adaptation of the Right Ventricle in Experimental Pulmonary Hypertension. ***Am J Respir Cell Mol Biol***. 2018;59:479-489.

56. Adair TH, Wells ML, Hang J, Montani JP. A stereological method for estimating length density of the arterial vascular system. ***Am J Physiol***. 1994;266:H1434-1438.

57. Graham BB, Koyanagi D, Kandasamy B, Tuder RM. Right Ventricle Vasculature in Human Pulmonary Hypertension Assessed by Stereology. ***Am J Respir Crit Care Med***. 2017;196:1075-1077.

58. Gomez-Arroyo J, Mizuno S, Szczepanek K, Van Tassell B, Natarajan R, dos Remedios CG, Drake JI, Farkas L, Kraskauskas D, Wijesinghe DS, Chalfant CE, Bigbee J, Abbate A, Lesnefsky EJ, Bogaard HJ, Voelkel NF. Metabolic gene remodeling and mitochondrial dysfunction in failing right ventricular hypertrophy secondary to pulmonary arterial hypertension. ***Circ Heart Fail***. 2013;6:136-144.

59. Piao L, Fang YH, Cadete VJ, Wietholt C, Urboniene D, Toth PT, Marsboom G, Zhang HJ, Haber I, Rehman J, Lopaschuk GD, Archer SL. The inhibition of pyruvate dehydrogenase kinase improves impaired cardiac function and electrical remodeling in two models of right ventricular hypertrophy: resuscitating the hibernating right ventricle. ***J Mol Med (Berl)***. 2010;88:47-60.

60. Kolb TM, Peabody J, Baddoura P, Fallica J, Mock JR, Singer BD, D'Alessio FR, Damarla M, Damico RL, Hassoun PM. Right Ventricular Angiogenesis is an Early Adaptive Response to Chronic Hypoxia-Induced Pulmonary Hypertension. ***Microcirculation***. 2015;22:724-736.

61. Potus F, Ruffenach G, Dahou A, Thebault C, Breuils-Bonnet S, Tremblay E, Nadeau V, Paradis R, Graydon C, Wong R, Johnson I, Paulin R, Lajoie AC, Perron J, Charbonneau E, Joubert P, Pibarot P, Michelakis ED, Provencher S, Bonnet S. Downregulation of microRNA-126 contributes to the failing right ventricle in pulmonary arterial hypertension. ***Circulation***. 2015;132:932-943.

62. Bogaard HJ, Natarajan R, Mizuno S, Abbate A, Chang PJ, Chau VQ, Hoke NN, Kraskauskas D, Kasper M, Salloum FN, Voelkel NF. Adrenergic receptor blockade reverses right heart remodeling and dysfunction in pulmonary hypertensive rats. ***Am J Respir Crit Care Med***. 2010;182:652-660.

63. Guo X, Li J, Zhang H, Liu H, Liu Z, Wei X. Relationship between ADAMTS8, ADAMTS18, and ADAMTS20 (a disintegrin and metalloproteinase with thrombospondin motifs) expressions and tumor molecular classification, clinical pathological parameters, and prognosis in breast invasive ductal carcinoma. ***Med Sci Monit***. 2018;24:3726-3735.

64. Gamen E, Seeger W, Pullamsetti SS. The emerging role of epigenetics in pulmonary hypertension. ***Eur Respir J***. 2016;48:903-917.

65. Larsen AR, Bai RY, Chung JH, Borodovsky A, Rudin CM, Riggins GJ, Bunz F. Repurposing the antihelmintic mebendazole as a hedgehog inhibitor. ***Mol Cancer Ther***. 2015;14:3-13.

66. Wang J, Wang H, Guo C, Luo W, Lawler A, Reddy A, Wang J, Sun EB, Eitzman DT. Mebendazole reduces vascular smooth muscle cell proliferation and neointimal formation following vascular injury in mice. ***PLoS One***. 2014;9:e90146.

67. Dunn JR, Reed JE, du Plessis DG, Shaw EJ, Reeves P, Gee AL, Warnke P, Walker C. Expression of ADAMTS-8, a secreted protease with antiangiogenic properties, is downregulated in brain tumours. ***Br J Cancer***. 2006;94:1186-1193.

68. Saleheen D, Zhao W, Young R, Nelson CP, Ho W, Ferguson JF, Rasheed A, Ou K, Nurnberg ST, Bauer RC, Goel A, Do R, Stewart AFR, Hartiala J, Zhang W, Thorleifsson G, Strawbridge RJ, Sinisalo

J, Kanoni S, Sedaghat S, Marouli E, Kristiansson K, Hua Zhao J, Scott R, Gauguier D, Shah SH, Smith AV, van Zuydam N, Cox AJ, Willenborg C, Kessler T, Zeng L, Province MA, Ganna A, Lind L, Pedersen NL, White CC, Joensuu A, Edi Kleber M, Hall AS, Marz W, Salomaa V, O'Donnell C, Ingelsson E, Feitosa MF, Erdmann J, Bowden DW, Palmer CNA, Gudnason V, Faire U, Zalloua P, Wareham N, Thompson JR, Kuulasmaa K, Dedoussis G, Perola M, Dehghan A, Chambers JC, Kooner J, Allayee H, Deloukas P, McPherson R, Stefansson K, Schunkert H, Kathiresan S, Farrall M, Marcel Frossard P, Rader DJ, Samani NJ, Reilly MP. Loss of cardioprotective effects at the ADAMTS7 locus as a result of gene-smoking interactions. ***Circulation***. 2017;135:2336-2353.

FIGURE LEGENDS

Figure 1. Screening for Novel Therapeutic Targets in PAH. (**A**) Primary culture of pulmonary artery smooth muscle cells (PASMCs) from patients with pulmonary arterial hypertension (PAH). (**B**) Volcano plots of gene expression variations in PAH-PASMCs and control PASMCs. The blue plot represents a probe for *ADAMTS8*. Dashed lines represent an adjusted P value of 0.05 and ± 1-fold change. Blue plots represent probes for ADAMTS8. (**C**) Domain structures of the ADAMTS family members. (**D**) Representative results of immunostaining of distal pulmonary arteries of PAH patients who underwent lung transplantation. Scale bars, 50 μm. (**E**) Representative results of immunofluorescence of distal pulmonary arteries of control and PAH patients. The smooth muscle layer is visualized by αSMA (Alexa Fluor-563, red). Double-immunostaining for ADAMTS8 (Alexa Fluor-488, green) and αSMA (red). Scale bars, 50 μm. (**F**) Representative Western blot and quantification of ADAMTS8 and tubulin in the lungs of control patients and those with PAH (*n*=6 each). (**G**) Real-time polymerase chain reaction (RT-PCR) analyses of *ADAMTS8* in PAH-PASMCs and control PASMCs (*n*=5 each). (**H**) Representative Western blot and the results of densitometric analysis of ADAMTS8 in PAH-PASMCs and control PASMCs (*n*=5 each). (**I**) RT-PCR analyses of *Adamts8* in tissues from normoxic and hypoxic (10% O_2, 4 weeks) mice (*n*=4–8). (**J, K**) Representative Western blot and results of densitometric analysis of ADAMTS8 in homogenates of the lung (**J**) and the heart (**K**) from normoxic and hypoxic (10% O_2, 4 weeks) mice (*n*=16–22). ADAMTS8, a disintegrin and metalloproteinase with thrombospondin motifs 8; PAH, pulmonary arterial hypertension; and PASMC, pulmonary artery smooth muscle cell. Results are expressed as mean±SEM. *P<0.05. The normality assumption was tested by Shapiro-Wilk Normality Test. Comparisons of means between 2 groups were performed by unpaired Student t test for normally distributed samples or Mann-Whitney U-test for not normally distributed samples.

Figure 2. PASMC-specific Deletion of ADAMTS8 Ameliorates Hypoxia-induced PH. (**A**) Schematic outline for generating vascular smooth muscle cell-specific ADAMTS8-knockout (ADAMTS8$^{\Delta SM22\alpha}$) mice. (**B**) Systolic blood pressure (SBP), diastolic blood pressure (DBP), heart rare (HR), and body weight in 8-week-old ADAMTS8$^{\Delta SM22}$ and control mice under normoxia (*n*=6 each). (**C**) Representative results of Elastica-Masson (EM) and immunostaining for α-smooth muscle actin (αSMA) of distal pulmonary arteries subjected to normoxia or hypoxia (10% O_2) for 4 weeks. Muscularization of the distal pulmonary arteries in ADAMTS8$^{\Delta SM22\alpha}$ and control mice subjected to normoxia (*n*=5 each) or hypoxia (10% O_2) for 4 weeks (*n*=10 each). N, non-muscularized vessels; P, partially muscularized vessels; F, fully muscularized vessels. Scale bars, 50 μm. (**D,E**) Right ventricular systolic pressure (RVSP) and right ventricular hypertrophy (RVH) in ADAMTS8$^{\Delta SM22\alpha}$ and control mice subjected to normoxia (*n*=5 each) or hypoxia (10% O_2) for 4 weeks (*n*=10 each). (**F**) Representative Western blots and quantification of ADAMTS8 protein levels in PASMCs from ADAMTS8$^{\Delta SM22\alpha}$ and control mice (*Adamts8*$^{-/-}$ PASMCs vs. *Adamts8*$^{+/+}$ PASMCs, *n*=4 each). (**G**) Proliferation of *Adamts8*$^{+/+}$ and *Adamts8*$^{-/-}$ PASMCs for 48 hours (*n*=8 each). (**H**) Representative pictures from wound healing assay in *Adamts8*$^{+/+}$ and *Adamts8*$^{-/-}$ PASMCs (*n*=6 each). †P < 0.05 compared with *Adamts8*$^{+/+}$ PASMCs. ADAMTS8, a disintegrin and metalloproteinase with thrombospondin motifs 8; PASMC, pulmonary artery smooth muscle cell; and PH, pulmonary hypertension. Results are expressed as mean±SEM. *P<0.05. The normality assumption was tested by Shapiro-Wilk Normality Test. Comparisons of means between 2 groups were performed by unpaired Student t test for normally distributed samples or Mann-Whitney U-test for not normally distributed samples. For multiple comparisons, two-way ANOVA (analysis of variance) followed by the Tukey HDS (honestly significant difference) method or the Dunnett's method for multiple comparison, as appropriate.

Figure 3. ADAMTS8 Promotes PASMC Proliferation. (**A**) Representative Western blots and quantification of phosphorylated AMPK at Thr17 (p-AMPK), total AMPK (t-AMPK), ACC phosphorylated at Ser79 (p-ACC), total ACC (t-ACC), Bcl-2, Bax, and PCNA in PASMCs from ADAMTS8$^{\Delta SM22\alpha}$ and control mice (*Adamts8*$^{-/-}$ PASMCs vs. *Adamts8*$^{+/+}$ PASMCs, *n*=6 each). (**B**) Proliferation of human PASMCs treated with human recombinant ADAMTS8 (hrADAMTS8) for 48 hours (*n*=8 each). (**C**) Representative Western blots and quantification of p-AMPK, t-AMPK, p-ACC, and t-ACC in human PASMCs treated with hrADAMTS8 for 24 hours (*n*=3 each). (**D**) Representative Western blots and quantification of Bcl-2 and Bax in human PASMCs treated with hrADAMTS8 (25 ng/mL) for 24 hours (*n*=3 each). (**E**) Real-time polymerase chain reaction (RT-PCR) analyses of *ADAMTS8*, *NOX4*, *CDKN1B*, *BAX*, and *APLN* mRNA in human PASMCs treated with human *ADAMTS8* plasmid DNA or control plasmid DNA for 48 hours (*n*=6 each). Average expression values are normalized to *GAPDH* mRNA. (**F**) RT-PCR analyses of *ADAMTS8*, *BAX*, *NOX4*, *CDKB1B*, *BCL2L11*, and *APLN* mRNA in human PASMCs

treated with control siRNA or ADAMTS8 siRNA for 48 hours (*n*=6 each). Average expression values are normalized to *GAPDH* mRNA. (**G**) Proliferation of human PASMCs treated with control siRNA or ADAMTS8 siRNA for 48 hours (*n*=8 each). AMPK, AMP-activated protein kinase; ACC, acetyl-CoA carboxylase; ADAMTS8, a disintegrin and metalloproteinase with thrombospondin motifs 8; PASMC, pulmonary artery smooth muscle cell; and PCNA, proliferating cell nuclear antigen. Results are expressed as mean±SEM. *P<0.05. The normality assumption was tested by Shapiro-Wilk Normality Test. Comparisons of means between 2 groups were performed by unpaired Student t test for normally distributed samples or Mann-Whitney U-test for not normally distributed samples. For multiple comparisons, one-way ANOVA (analysis of variance) for normally distributed samples followed by the Tukey HDS (honestly significant difference) method or the Dunnett's method for multiple comparison, as appropriate. The multiple comparison for not normally distributed samples was performed with Kruskal-Wallis test.

Figure 4. ADAMTS8-mediated Mitochondrial Dysfunction in PASMCs. (**A**) Quantification of 2,7-dichlorodihydrofluorescein (DCF) fluorescence intensity in *Adamts8*$^{+/+}$ and *Adamts8*$^{-/-}$ PASMCs after exposure to normoxia (21% O_2) or hypoxia (1% O_2) for 48 hours (*n*=8 each). (**B**) Representative images of CellROX staining and quantitative analysis of CellROX fluorescence intensity in *Adamts8*$^{+/+}$ and *Adamts8*$^{-/-}$ PASMCs under normoxia (21% O_2) or hypoxia (1% O_2) for 48 hours (*n*=4 each). Scale bars, 25 μm. (**C**) Quantification of MitoSOX fluorescence intensity in *Adamts8*$^{+/+}$ and *Adamts8*$^{-/-}$ PASMCs under normoxia (21% O_2) or hypoxia (1% O_2) for 48 hours (*n*=8 each). (**D**) Left, representative images of dihydroethidium (DHE) staining of pulmonary arteries from ADAMTS8$^{\Delta SM22\alpha}$ and control mice after hypoxic exposure (10% O_2) for 28 days. Right, quantification of DHE fluorescence intensity within autofluorescence of the elastic lamina in the distal pulmonary arteries from ADAMTS8$^{\Delta SM22\alpha}$ and control mice after hypoxic exposure (10% O_2) for 0, 3, 7, and 28 days (*n*=5 each). Scale bars, 50 μm. #P<0.05 compared with normoxic control mice. ¶P<0.05 compared with normoxic ADAMTS8$^{\Delta SM22\alpha}$ mice. (**E**) Representative images of *Adamts8*$^{+/+}$ and *Adamts8*$^{-/-}$ PASMCs after normoxia (21% O_2) or hypoxia (1% O_2) for 48 hours (*n*=4 each) labeled for mitochondria. Nuclei were counter-stained using DAPI. Scale bars, 20 μm. (**F**) Representative Western blots and quantification of DRP-1 (p-DRP-1) phosphorylated at Ser637 and total DRP-1 (t-DRP-1) in *Adamts8*$^{+/+}$ and *Adamts8*$^{-/-}$ PASMCs (*n*=6 each). (**G**) Real-time polymerase chain reaction (RT-PCR) analyses of *Mfn1* and *Mfn2* mRNA in *Adamts8*$^{+/+}$ and *Adamts8*$^{-/-}$ PASMCs (*n* = 6 each). Average expression values are normalized to *Gapdh* mRNA. (**H**) RT-PCR analyses of *Fis1* and *Mff* mRNA in *Adamts8*$^{+/+}$ and *Adamts8*$^{-/-}$ PASMCs (*n*=6 each). Average expression values are normalized to *Gapdh* mRNA. (**I**) Representative transmission electron microscopy images of mitochondria in smooth muscle layers of pulmonary arteries from ADAMTS8$^{\Delta SM22\alpha}$ and control mice subjected to normoxia (21% O_2) or hypoxia (10% O_2) for 4 weeks. The arrows indicate mitochondria. Scale bars, 1 μm. (**J**) Quantification of

NADPH oxidase activity in *Adamts8*$^{+/+}$ and *Adamts8*$^{-/-}$ PASMCs after exposure to normoxia (21% O_2) or hypoxia (1% O_2) for 48 hours (*n*=8 each). DRP-1, dynamin-related protein 1; ADAMTS8, a disintegrin and metalloproteinase with thrombospondin motifs 8; PASMC, pulmonary artery smooth muscle cell; ROS, reactive oxygen species; NADPH, nicotinamide adenine dinucleotide phosphate; and NOX4, NADPH oxidase 4. Results are expressed as mean±SEM. *P<0.05. The normality assumption was tested by Shapiro-Wilk Normality Test. Comparisons of means between 2 groups were performed by unpaired Student t test for normally distributed samples or Mann-Whitney U-test for not normally distributed samples. For multiple comparisons, one-way ANOVA (analysis of variance) for normally distributed samples followed by the Tukey HDS (honestly significant difference) method or the Dunnett's method for multiple comparison, as appropriate. The multiple comparison for not normally distributed samples was performed with Kruskal-Wallis test.

Figure 5. ADAMTS8 Promotes MMP Activation. (**A**) Gelatin zymography detection of pro-MMP-2, MMP-2, pro MMP-9 and MMP-9 in conditioned medium (CM) from human PASMCs treated with human recombinant ADAMTS8 (hrADAMTS8) for 24 hours (*n*=3 each). (**B**) Representative Western blots and quantification of cyclophilin A (CyPA) and basigin (Bsg) in conditioned medium (CM) and total cell lysate (TCL) of human PASMCs treated with hrADAMTS8 (25 ng/mL) for 24 hours (*n*=3 each). (**C**) Representative images of in situ zymography (DQ gelatin) in *Adamts8*$^{+/+}$ and *Adamts8*$^{-/-}$ PASMCs after exposure to normoxia (21% O_2) or hypoxia (1% O_2) for 48 hours. Nuclei were counter-stained using DAPI. Scale bars, 20 μm. Quantification of DQ gelatin fluorescence intensity in *Adamts8*$^{+/+}$ and *Adamts8*$^{-/-}$ PASMCs under normoxia (21% O_2) or hypoxia (1% O_2) for 48 hours (*n*=8 each). (**D**) Left, representative results of in situ zymography and immunostaining for αSMA of the distal pulmonary arteries in ADAMTS8$^{\Delta SM22\alpha}$ and control mice subjected to normoxia or hypoxia (10% O_2) for 0, 3, 7, and 28 days. Right, quantitation of MMP activity in the αSMA-positive area in distal pulmonary arteries of ADAMTS8$^{\Delta SM22\alpha}$ control mice subjected to hypoxia (10% O_2) for 28 days (*n*=5 each). Scale bars, 25 μm. #P<0.05 compared with normoxic control mice. ¶P < 0.05 compared with normoxic ADAMTS8$^{\Delta SM22\alpha}$ mice. (**E**) Real-time polymerase chain reaction (RT-PCR) analyses of *Mmp-2* mRNA in lung homogenates from ADAMTS8$^{\Delta sm22}$ and control mice subjected to normoxia (*n*=4 each) or hypoxia (10% O_2) for 0, 3, 7, and 28 days (*n*=8 each). Average expression levels are normalized to *Gapdh* mRNA. #P<0.05 compared with normoxic control mice. ¶P<0.05 compared with normoxic ADAMTS8$^{\Delta SM22\alpha}$ mice. MMP, matrix metalloproteinase; ADAMTS8, a disintegrin and metalloproteinase with thrombospondin motifs 8; ECM, extracellular matrix; and PASMC, pulmonary artery smooth muscle cell. Results are expressed as mean±SEM. *P<0.05. The normality assumption was tested by Shapiro-Wilk Normality Test. Comparisons of means between 2 groups were performed by unpaired Student t test for normally distributed samples or

Mann-Whitney U-test for not normally distributed samples. For multiple comparisons, one-way ANOVA (analysis of variance) for normally distributed samples followed by the Tukey HDS (honestly significant difference) method or the Dunnett's method for multiple comparison, as appropriate. The multiple comparison for not normally distributed samples was performed with Kruskal-Wallis test.

Figure 6. ADAMTS8-mediated Interaction Between PASMCs and PAECs. (**A**) Representative Western blots and quantification of VEGF receptor 2 phosphorylated at Tyr951 (p-VEGFR2) and total VEGF receptor 2 (t-VEGFR2) in human PAECs treated with human recombinant ADAMTS8 (hrADAMTS8 1 μg/mL, 15 min) followed by VEGF-A stimulation (25 ng/mL, 15 min, *n*=3 each). (**B**) Representative Western blots and quantification of AMPK phosphorylated at Thr17 (p-AMPK), total AMPK (t-AMPK), ACC phosphorylated at Ser79 (p-ACC), and total ACC (t-ACC) in human PAECs treated with hrADAMTS8 (1 μg/mL) for 24 hours followed by AICAR stimulation for 2 hours (1 mmol/L, *n*=6 each). (**C**) Proliferation of human PAECs during treatment with hrADAMTS8 (0.025 μg/mL, 1 μg/mL and 5 μg/mL) for 48 hours (*n*=8 each). (**D**) Treatment of human PAECs with conditioned medium (CM) from control plasmid-transfected PASMCs (Control-CM) or ADAMTS8 plasmid-transfected PASMCs (ADAMTS8-CM). (**E**) Representative Western blots and quantification of p-AMPK and total AMPK in human PAECs treated with Control-CM or ADAMTS8-CM for 24 hours (*n*=6 each). (**F**) Representative pictures from the tube formation assay and quantitative analysis in human PAECs treated with Control-CM or ADAMTS8-CM for 8 hours (*n*=6 each). Scale bars, 100 μm. (**G**) Representative images of CellROX and quantitative analysis of CellROX fluorescence intensity in human PAECs treated with Control-CM or ADAMTS8-CM for 24 hours (*n*=4 each). Scale bars, 25 μm. (**H**) Real-time polymerase chain reaction (RT-PCR) analyses of *BAX, CCND1*, and *APLN* mRNA in human PAECs treated with Control-CM or ADAMTS8-CM for 24 hours (*n*=6 each). Average expression levels are normalized to *GAPDH* mRNA. (**I**) Schematic representation of molecular mechanisms of ADAMTS8-mediated interaction between PASMCs and PAECs. ADAMTS8, a disintegrin and metalloproteinase with thrombospondin motifs 8; CCND1, Cyclin D1; VEGF, vascular endothelial growth factor; PAEC, pulmonary artery endothelial cell; AMPK, AMP-activated protein kinase; ACC, acetyl-CoA carboxylase; and PASMC, pulmonary artery smooth muscle cell. Results are expressed as mean±SEM. *P<0.05. The normality assumption was tested by Shapiro-Wilk Normality Test. Comparisons of means between 2 groups were performed by unpaired Student t test for normally distributed samples or Mann-Whitney U-test for not normally distributed samples. For multiple comparisons, one-way ANOVA (analysis of variance) for normally distributed samples followed by the Tukey HDS (honestly significant difference) method or the Dunnett's method for multiple comparison, as appropriate. The multiple comparison for not normally distributed samples was performed with Kruskal-Wallis test.

Figure 7. Cardiomyocyte-specific Deletion of ADAMTS8 Ameliorates RV Failure. (**A**) Schematic outline for generating cardiomyocyte-specific ADAMTS8 knockout (ADAMTS8$^{\Delta\alpha MHC}$) mice. (**B**) Quantification of protein levels of ADAMTS8 in the hearts of ADAMTS8$^{\Delta\alpha MHC}$ and control mice (*n*=4 each). (**C**) RV systolic pressure (RVSP) and RV hypertrophy (RVH) in ADAMTS8$^{\Delta\alpha MHC}$ and control mice subjected to normoxia (*n*=6 each) or hypoxia (10% O_2) for 4 weeks (*n*=10 each). (**D**) Walking distance, assessed by a treadmill test, in ADAMTS8$^{\Delta\alpha MHC}$ and control mice subjected to normoxia (*n*=6 each) or hypoxia (10% O_2) for 4 weeks (*n*=10 each). (**E**) Quantitative analyses of the parameters of RV function in ADAMTS8$^{\Delta\alpha MHC}$ and control mice subjected to normoxia (*n*=6 each) or hypoxia (10% O_2) for 4 weeks (*n*=10 each). (**F**) Representative pictures from sirius red staining and quantitative analysis of interstitial fibrotic area in RVs of ADAMTS8$^{\Delta\alpha MHC}$ and control mice subjected to normoxia or hypoxia (10% O_2) for 4 weeks (*n*=6 each). Scale bars, 25 μm. (**G**) Representative immunostaining pictures of RVs and quantitative analysis of capillary density in ADAMTS8$^{\Delta\alpha MHC}$ and control mice subjected to normoxia or hypoxia (10% O_2) for 4 weeks (*n*=6 each). Scale bars, 25 μm. (**H**) Representative results of immunostaining for pimonidazole for detection of myocardial hypoxia in RVs. Quantitative analysis of the myocardial hypoxic area in RVs from ADAMTS8$^{\Delta\alpha MHC}$ and control mice subjected to normoxia or hypoxia (10% O_2) for 4 weeks (*n*=6 each). Scale bars, 100 μm. (**I**) Real-time polymerase chain reaction (RT-PCR) analyses of *Anf*, *Bnp*, *Col3a*, and *Glut4* mRNA in RVs from ADAMTS8$^{\Delta\alpha MHC}$ and control mice subjected to normoxia (*n*=6 each) or hypoxia (10% O_2) for 4 weeks (*n*=12 each). Average expression levels are normalized to *Gapdh* mRNA. ADAMTS8, a disintegrin and metalloproteinase with thrombospondin motifs 8; PH, pulmonary hypertension; RV, right ventricular; VTI, velocity time integral; AcT, acceleration time; ET, ejection time; TAPSE, tricuspid annular plane systolic excursion; CO, cardiac output; and RVID, RV internal diameter. Results are expressed as mean±SEM. *P<0.05. The normality assumption was tested by Shapiro-Wilk Normality Test. Comparisons of means between 2 groups were performed by unpaired Student t test for normally distributed samples or Mann-Whitney U-test for not normally distributed samples. For multiple comparisons, two-way ANOVA (analysis of variance) for normally distributed samples followed by the Tukey HDS (honestly significant difference) method.

Figure 8. Mebendazole Ameliorates PH in Animal Models *in Vivo*. (**A**) Schematic outline of high-throughput screening (HTS) to identify compounds that suppress *ADAMTS8* expression and proliferation in PASMCs from patients with PAH (PAH-PASMCs). First, we treated PAH-PASMCs with 3,336 compounds (5 μmol/L each) for 48 hours and performed a proliferation assay (MTT assay). We identified 113 compounds that suppressed PAH-PASMC proliferation by more than 20%. We then treated PAH-PASMCs with these 113 compounds (5 μmol/L each) for 4 hours and measured *ADAMTS8* expression by

RT-PCR using extracted total RNA, resulting in identification of 31 compounds that suppress *ADAMTS8* mRNA expression. Drugs approved in clinical settings were selected for further analysis. Finally, we examined the effects of 3 compounds in mice with hypoxia-induced pulmonary hypertension (PH) for validation. (**B**) Results for the 31 compounds that suppress PAH-PASMC proliferation (gray bars) and *ADAMTS8* gene expression (red plots). (**C**) Representative Western blots and quantification of ADAMTS8 in PAH-PASMCs treated with mebendazole (5 μmol/L) for 48 hours (*n*=6 each). (**D**) Proliferation of PAH-PASMCs cultured in 5% fetal bovine serum with mebendazole (0.5, 5, or 10 μmol/L) for 24 hours (vehicle, *n*=16; mebendazole, *n*=8 each). (**E**) Representative Western blot and quantification of ADAMTS8 protein levels in the lung and RVs of rats subjected to chronic hypoxia for 21 days in combination with administration of a VEGF receptor blocker SU5416 (Sugen/hypoxia rats) followed by treatment with vehicle or mebendazole for 14 days after induction of PAH. (**F**) RV systolic pressure (RVSP) and RV hypertrophy (RVH) in Sugen/hypoxia rats as a result of treatment with vehicle or mebendazole for 14 days after induction of PAH. (**G**) Left, representative results of Elastica-Masson (EM) and immunostaining for α-smooth muscle actin (αSMA) of distal pulmonary arteries in the lungs from Sugen/hypoxia rats treated with vehicle or mebendazole for 14 days after induction of PAH. Right, quantitative analysis of medial wall thickness of pulmonary arteries with a diameter of 50 to 100 μm. Scale bars, 50 μm. (**H**) Left, representative images of immunostaining of RVs from Sugen/hypoxia rats treated with vehicle or mebendazole for 14 days after induction of PAH. Right, quantitative analysis of capillary density in RVs. Scale bars, 25 μm. (**I**) Left, representative pictures of sirius red staining of the RVs from Sugen/hypoxia rats treated with vehicle or mebendazole for 14 days after induction of PAH. Right, quantitative analysis of the interstitial fibrotic area in the RVs. Scale bars, 25 μm. (**J**) Walking distance in Sugen/hypoxia rats treated with vehicle or mebendazole. (**K**) Schematic representation of molecular mechanisms of ADAMTS8-mediated pulmonary vascular remodeling and RV dysfunction. ADAMTS8, a disintegrin and metalloproteinase with thrombospondin motifs 8; PH, pulmonary hypertension; RV, right ventricle; PAH, pulmonary arterial hypertension; PASMC, pulmonary artery smooth muscle cell; and MTT, 3-(4,5-di-methylthiazol-2-yl)-2,5-diphenyltetrazolium bromide. *n*=5 for control rats (rats that did not receive SU5416 injection or were subjected to chronic hypoxia), *n*=10 for vehicle or mebendazole-treated rats per group. Results are expressed as mean±SEM. *P<0.05. The normality assumption was tested by Shapiro-Wilk Normality Test. Comparisons of means between 2 groups were performed by unpaired Student t test for normally distributed samples or Mann-Whitney U-test for not normally distributed samples. For multiple comparisons, one-way ANOVA (analysis of variance) for normally distributed samples followed by the Tukey HDS (honestly significant difference) method. The multiple comparison for not normally distributed samples was performed with Kruskal-Wallis test.

NOVELTY AND SIGNIFICANCE

What Is Known?

- Pulmonary arterial hypertension (PAH) is characterized by pulmonary vascular remodeling with aberrant pulmonary artery smooth muscle cell (PASMC) proliferation, endothelial dysfunction, and extracellular matrix (ECM) remodeling.
- Right ventricular (RV) function is an important prognostic factor in PAH.

What New Information Does This Article Contribute?

- A disintegrin and metalloproteinase with thrombospondin motifs 8 (ADAMTS8), a secreted protein, was up-regulated in PASMCs from PAH patients (PAH-PASMCs).
- ADAMTS8 promoted proliferation of PASMCs, ECM remodeling, and endothelial dysfunction in an autocrine/paracrine manner.
- The depletion of ADAMTS8 improved PH and RV dysfunction in rodent models of pulmonary hypertension (PH).
- Mebendazole, an anthelmintic drug, reduced ADAMTS8 expression in PASMCs and their proliferation and ameliorated PH and RV dysfunction in rodent models of PH.

This is the first study that demonstrates the pathogenic role of ADAMTS8 in PAH. Based on the findings of the present study, the up-regulation of ADAMTS8 in PASMCs from PAH patients (PAH-PASMCs) contributed to the aberrant cell proliferation of PASMCs and ECM remodeling. Mechanistic analysis demonstrated ADAMTS8 induced numerous intracellular signals to promote cell proliferation of PASMCs accompanied by activation of extracellular matrix metalloproteinases and NOX4-mediated ROS production. Moreover, ADAMTS8 secreted from adjacent PASMCs induced endothelial dysfunction in an autocrine/paracrine manner through down-regulation of VEGFR2/AMPK signaling. Additionally, we demonstrated the depletion of ADAMTS8 attenuated pulmonary hypertension (PH) and RV failure in rodent animal models of PH. These findings suggested that these integrated effects caused by the up-regulation of ADAMTS8 in PASMCs may promote the pathogenesis of PAH. Next, using high-throughput screening, we discovered that mebendazole, an anthelmintic drug, reduced ADAMTS8 expression in PASMCs and their proliferation. Finally, we demonstrated that mebendazole ameliorated PH and RV dysfunction in rodent models of PH associated with down-regulation of ADAMTS8. Based on these findings, we identify ADAMTS8 as a therapeutic target for PAH and propose a possibility of drug repositioning in mebendazole as PAH treatment.

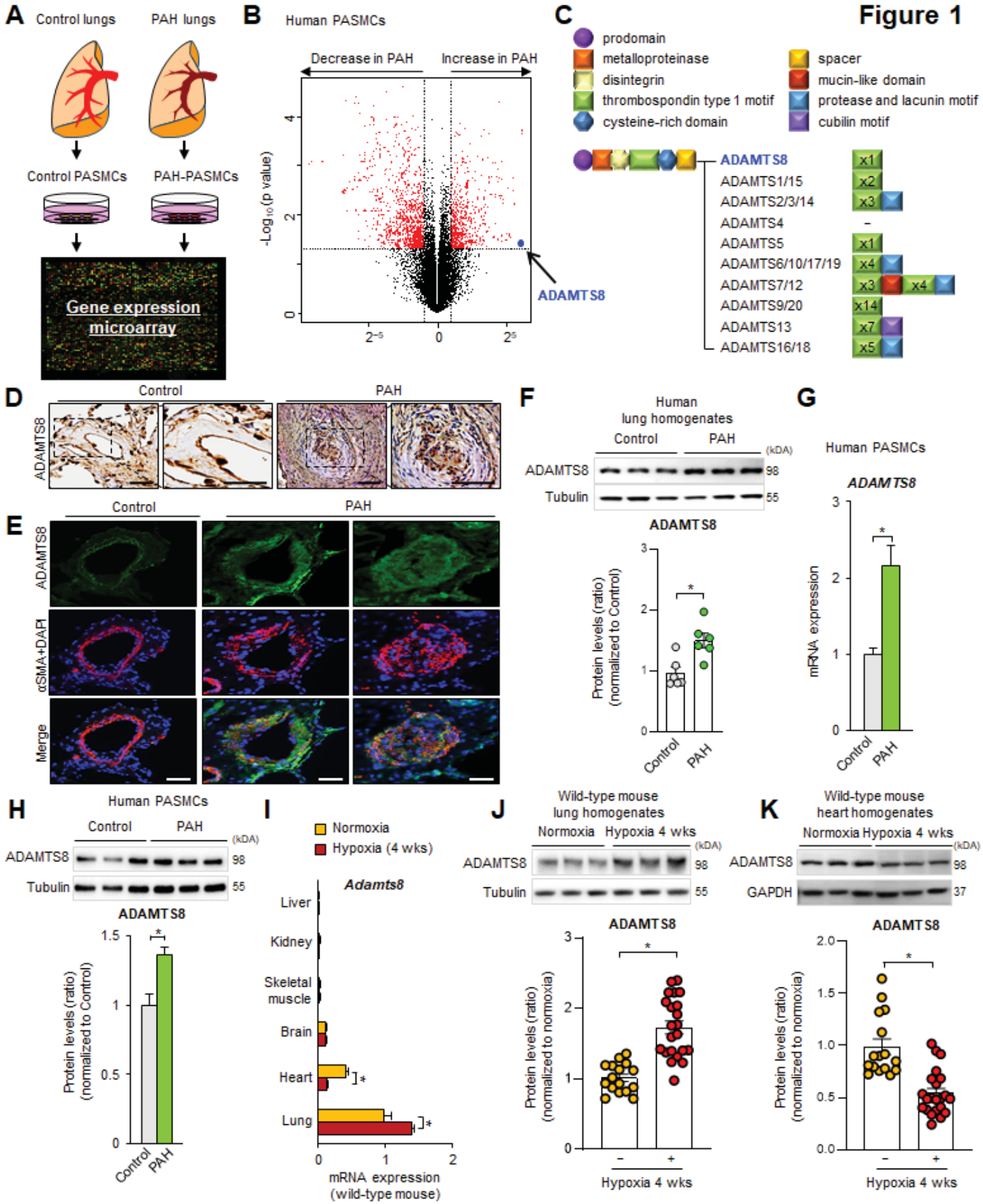

Figure 2

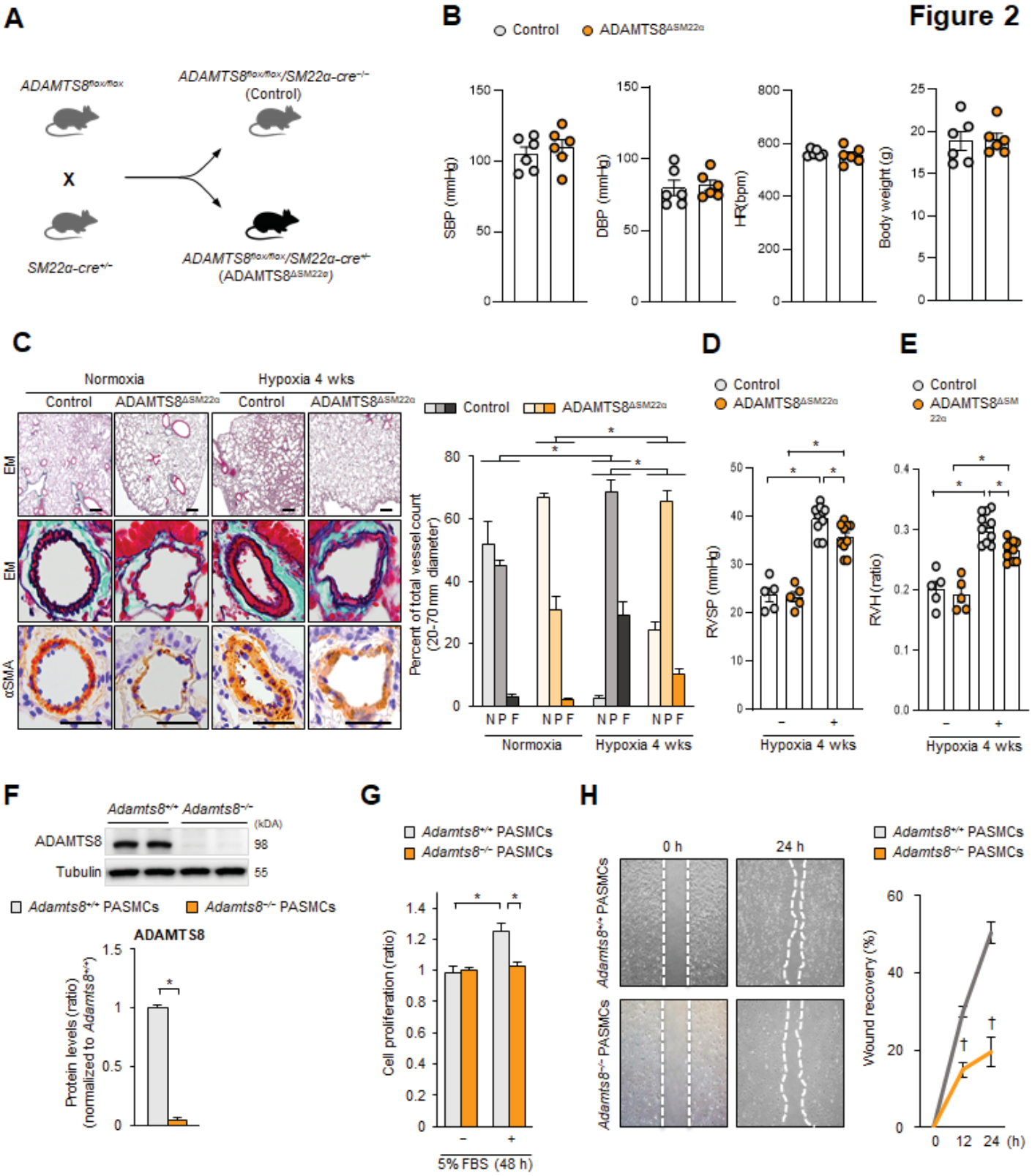

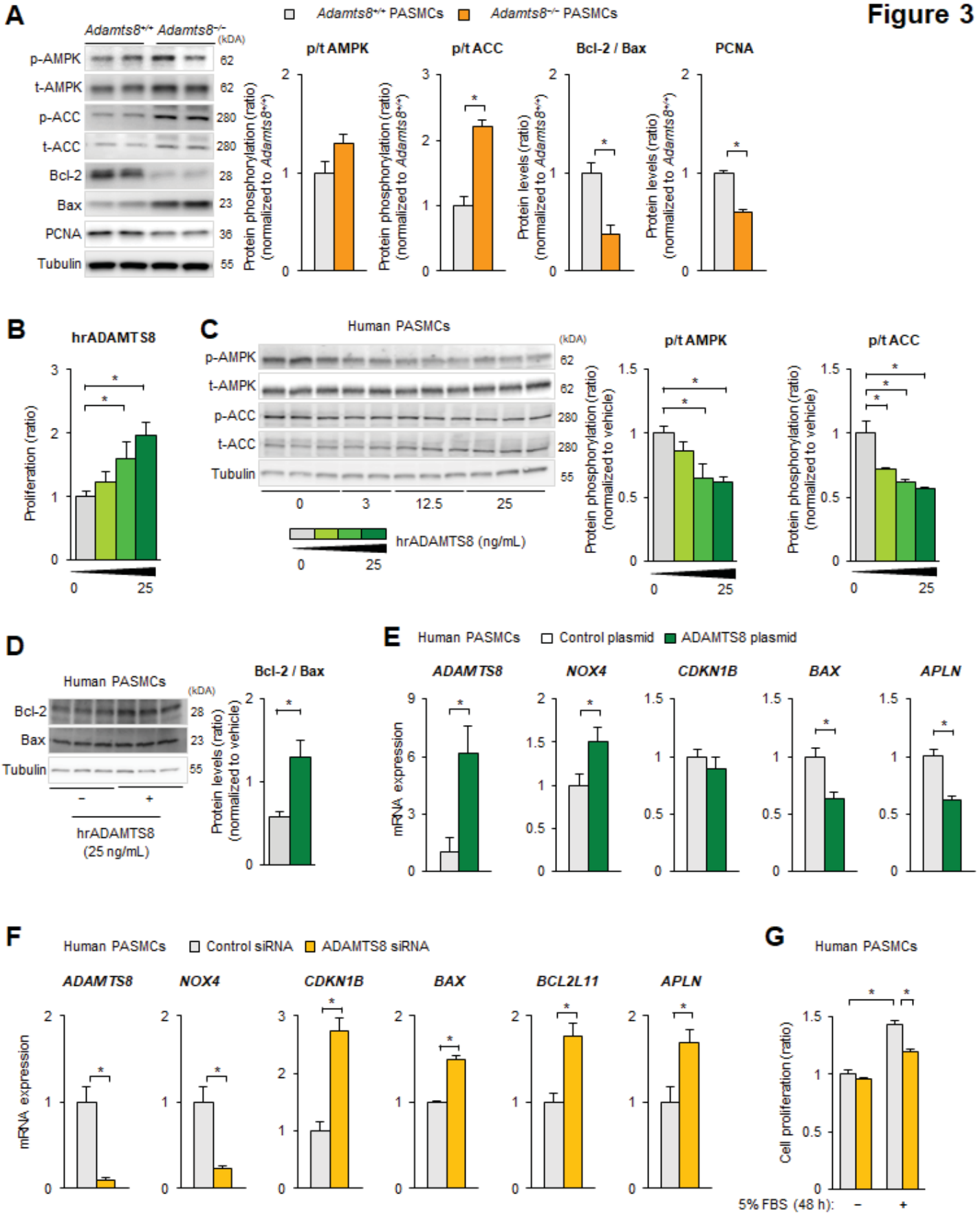

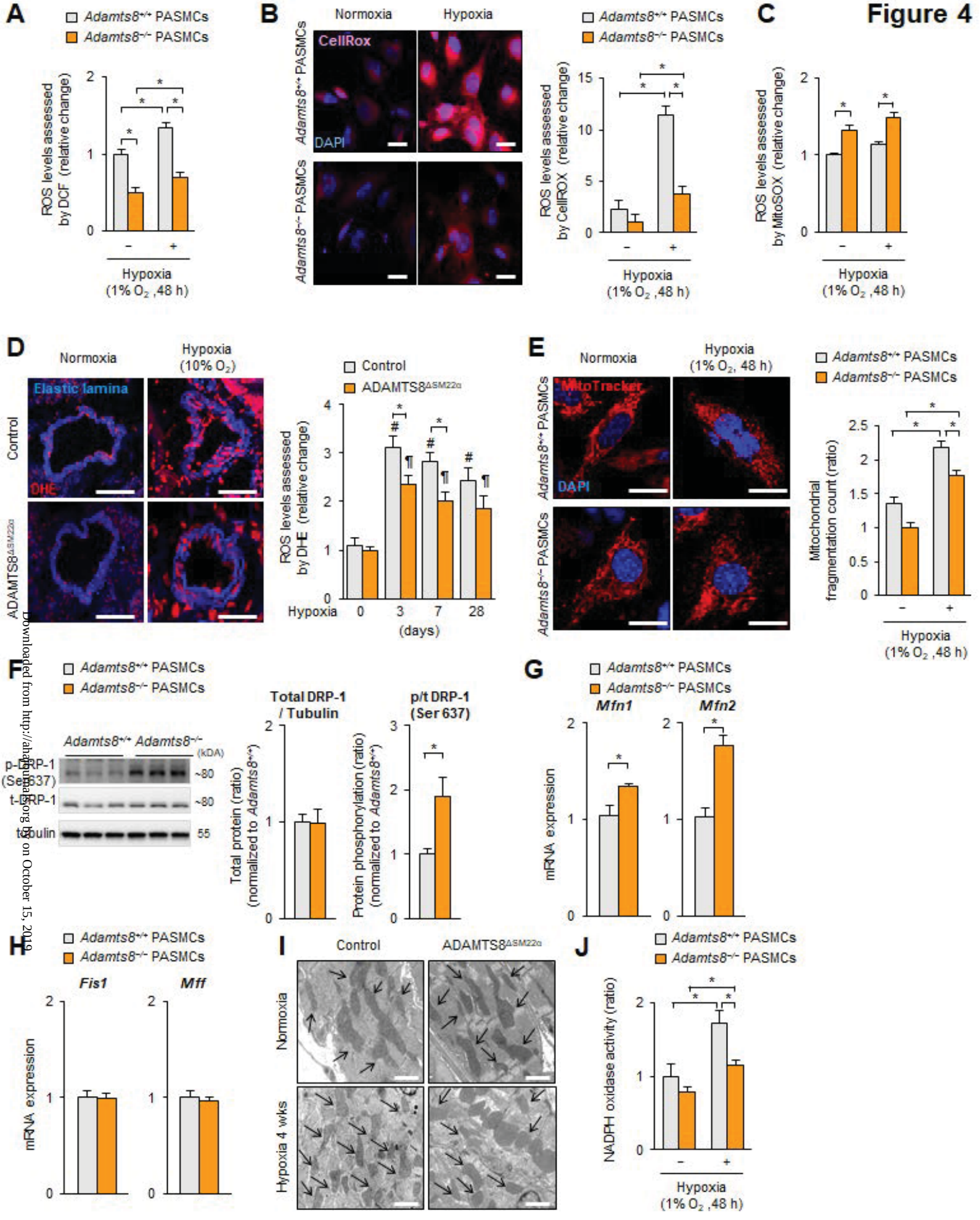

Figure 5